16th SPIE Int'l Symposium on Smart Structures and Materials

Nano-Bio Quantum Technology for Device Specific Materials

Sang H. Choi

Advanced Materials and Processing Branch
NASA Langley Research Center

March 9-12, 2009

POC: 757-864-1408, Sang.H.Choi@NASA.GOV

Areas to be discussed

- Thermoelectric Materials
- Smart Optical Materials
  - Quantum Apertures
  - Micro Spectrometers
  - Light Control Ferroelectric Materials
- Ferritin Molecules
  - Biotemplates for Nanopartices
  - Bionanobattery

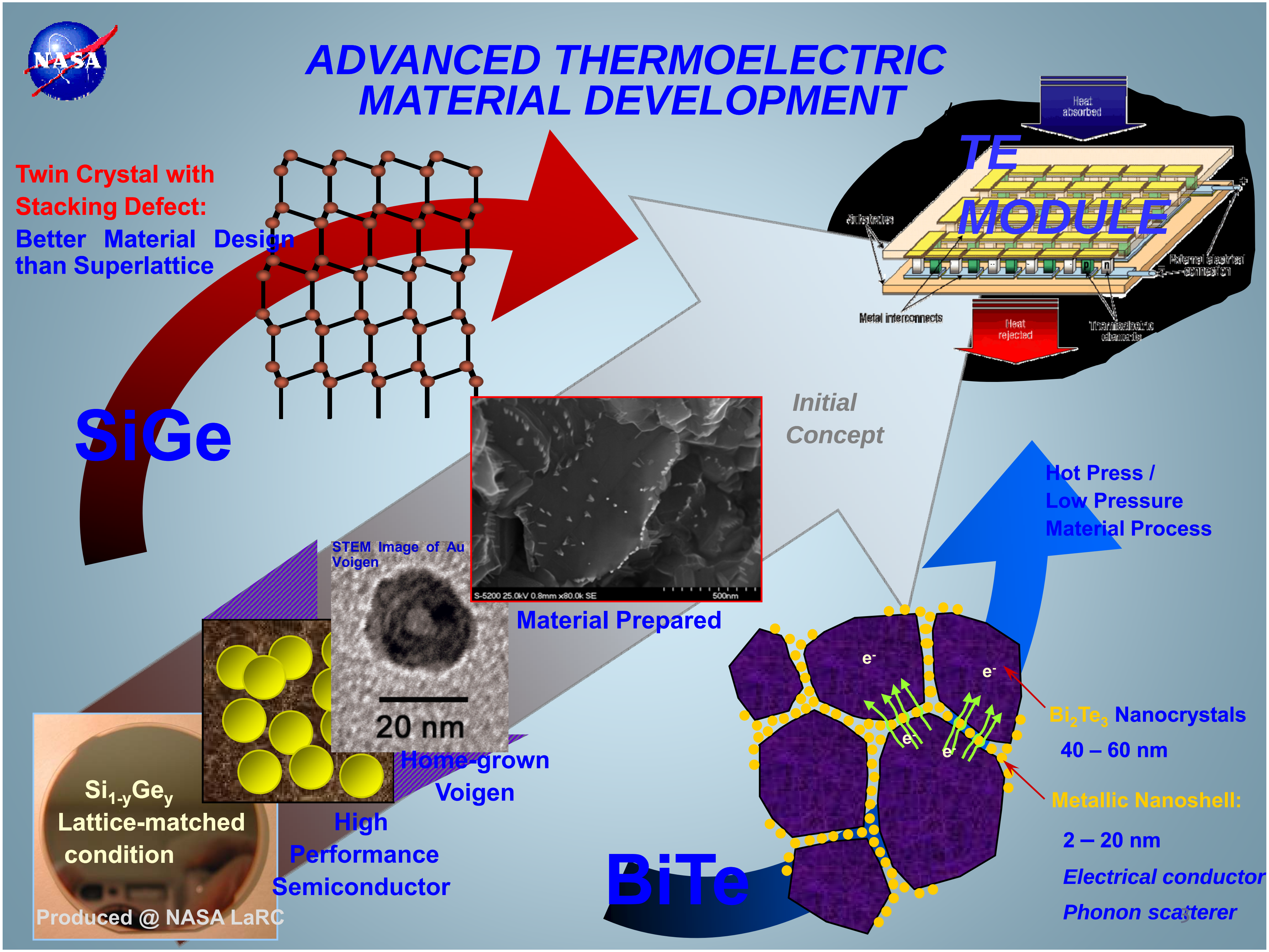

ADVANCED THERMOELECTRIC MATERIAL DEVELOPMENT
NASA
Twin Crystal with Stacking Defect:
Better Material Design than Superlattice
SiGe
Heat absorbed
TE MODULE
Substrates
External electrical connection
Metal interconnects
Heat rejected
Thermoelectric elements
Initial Concept
S-5200 25.0kV 0.8mm x80.0k SE 500nm
Material Prepared
Hot Press / Low Pressure Material Process
STEM Image of Au Voigen
20 nm
Home-grown Voigen
High Performance Semiconductor
$Si_{1-y}Ge_y$ Lattice-matched condition
Produced @ NASA LaRC
BiTe
e^-
Bi_2Te_3 Nanocrystals
40 – 60 nm
Metallic Nanoshell:
2 – 20 nm
Electrical conductor
Phonon scatterer

TE Performance Summary: Results & Projections

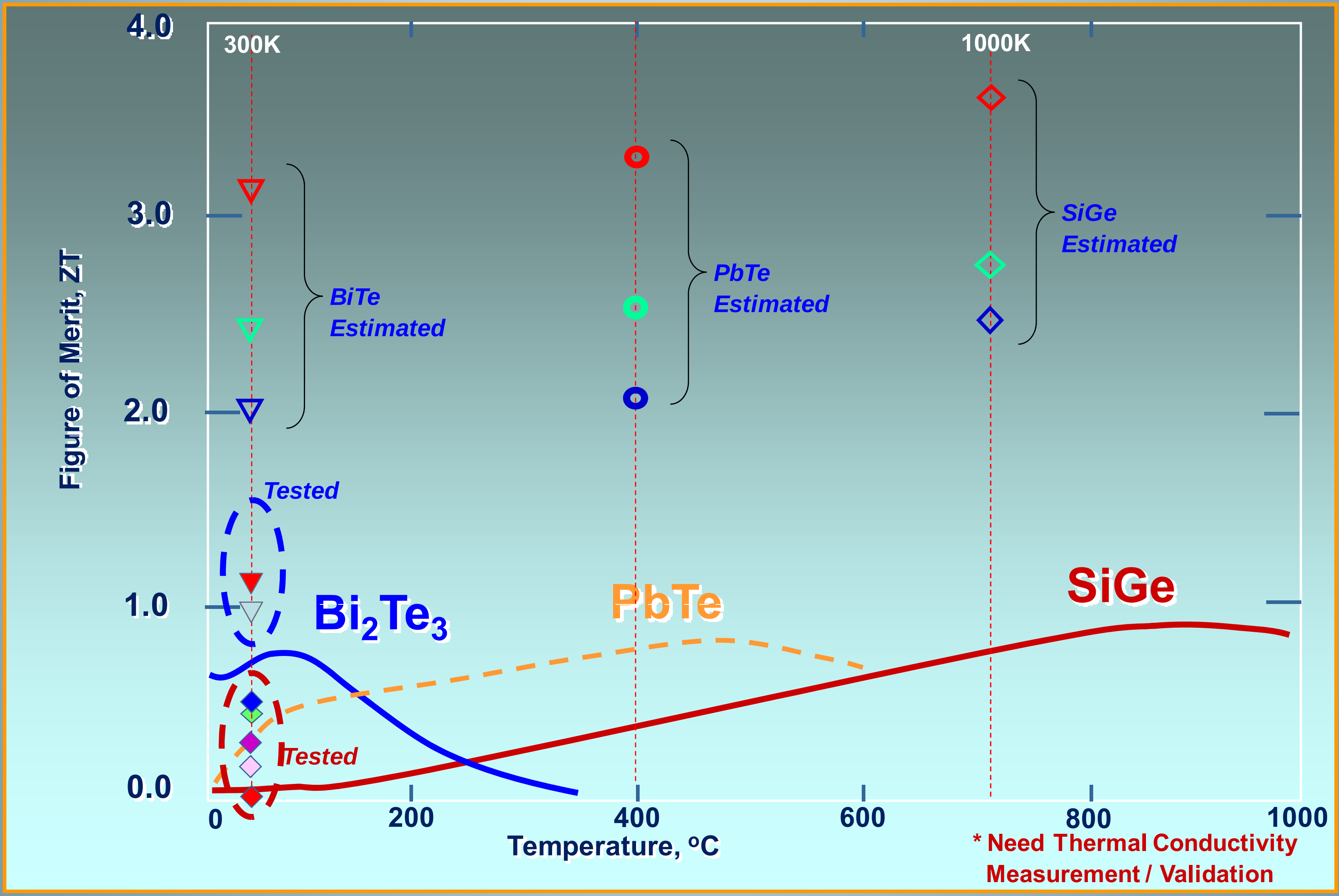

ATE Device for Solar Energy Conversion

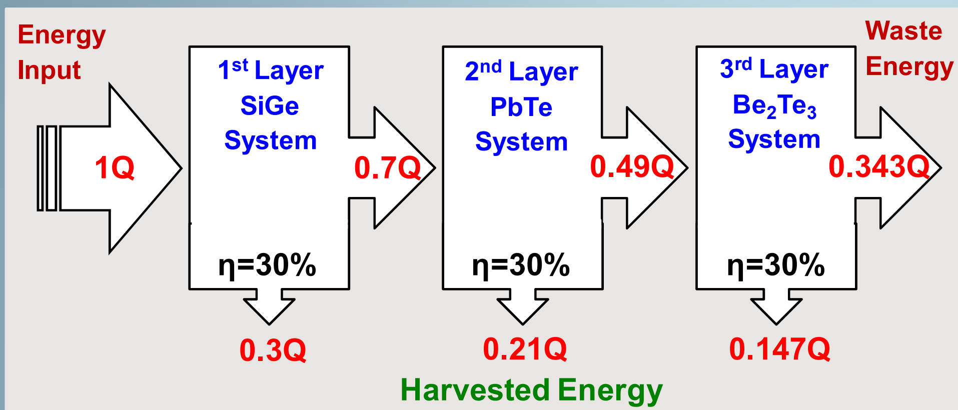

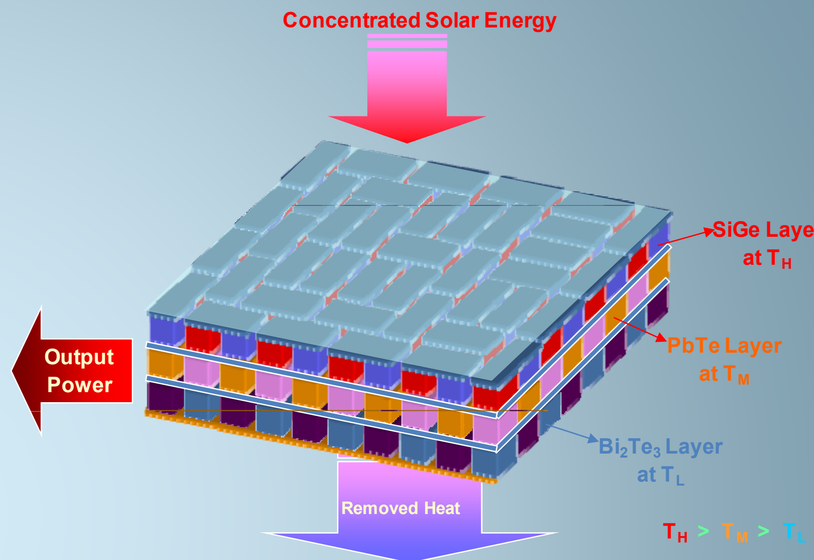

TE Tandem System	TE FoM ≥ 1.5 η = 10%		TE FoM ≥ 3.5 η = 20%		TE FoM ≥ 4.5 η = 30%		Solar Cells
	Loaded Energy, Q	η	Loaded Energy, Q	η	Loaded Energy, Q	η	η
1st Layer (Hi T)	1Q in 0.9Q out	10 %	1Q in 0.8Q out	20 %	1Q in 0.7Q out	30 %	30 % (?) for membrane PV
2nd Layer (Med T)	0.9 in 0.81Q out	10 %	0.8 in 0.64Q out	20 %	0.7 in 0.49Q out	30 %	
3rd Layer (Low T)	0.81Q in 0.729Q out	10 %	0.64Q in 0.512Q out	20 %	0.49Q in 0.343Q out	30 %	
Cascade Efficiency	0.271Q Harvested	27 %	0.488Q Harvested	48 %	0.657Q Harvested	65 %	

Si-Ge: Twin-Lattice Structure

Symmetry Breaking to 60:40

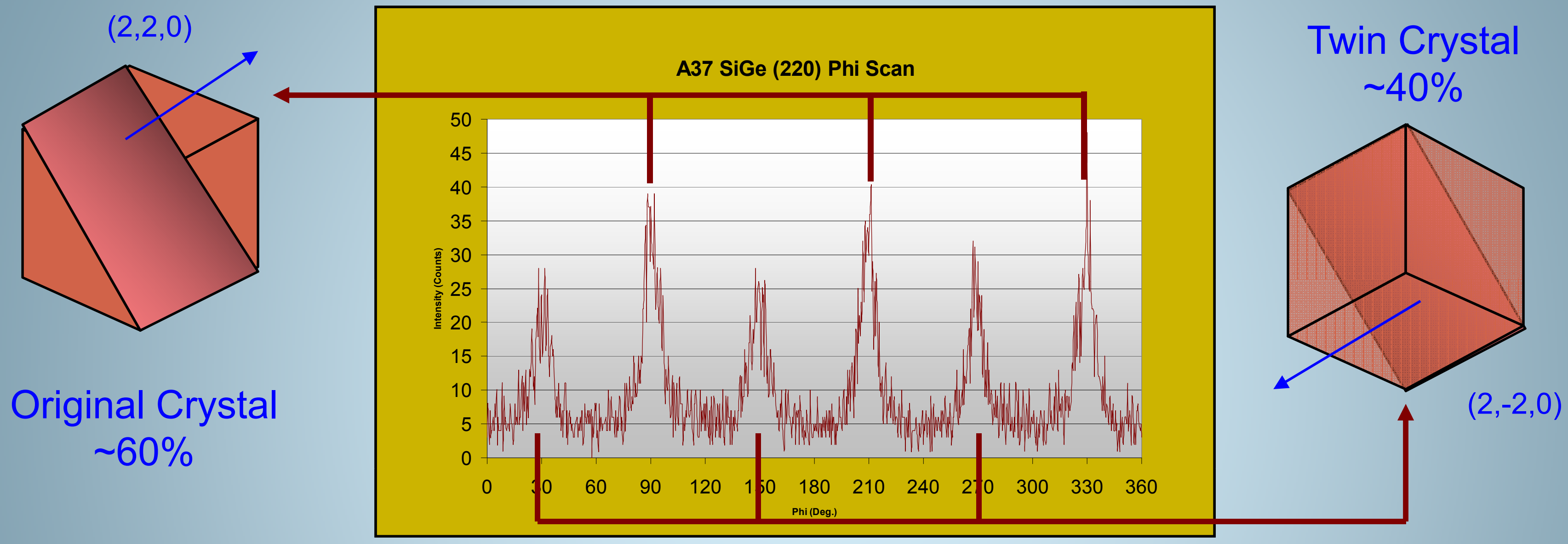

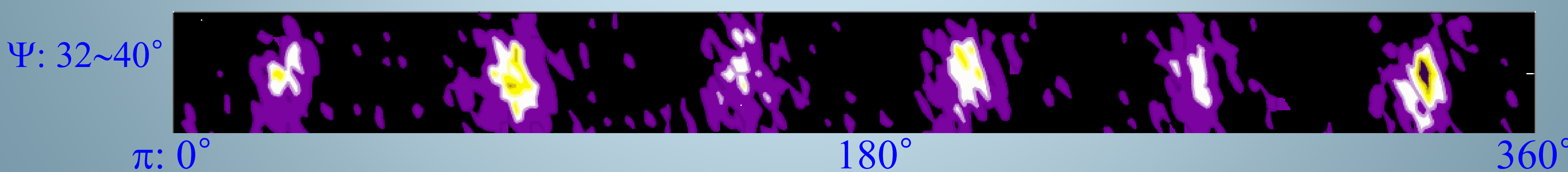

Rhombohedral Hybrid Band-Gap Engineering

Two Single Crystalline Alignments

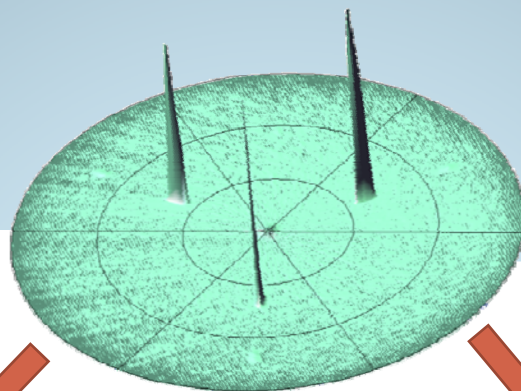

Sapphire {10-14}

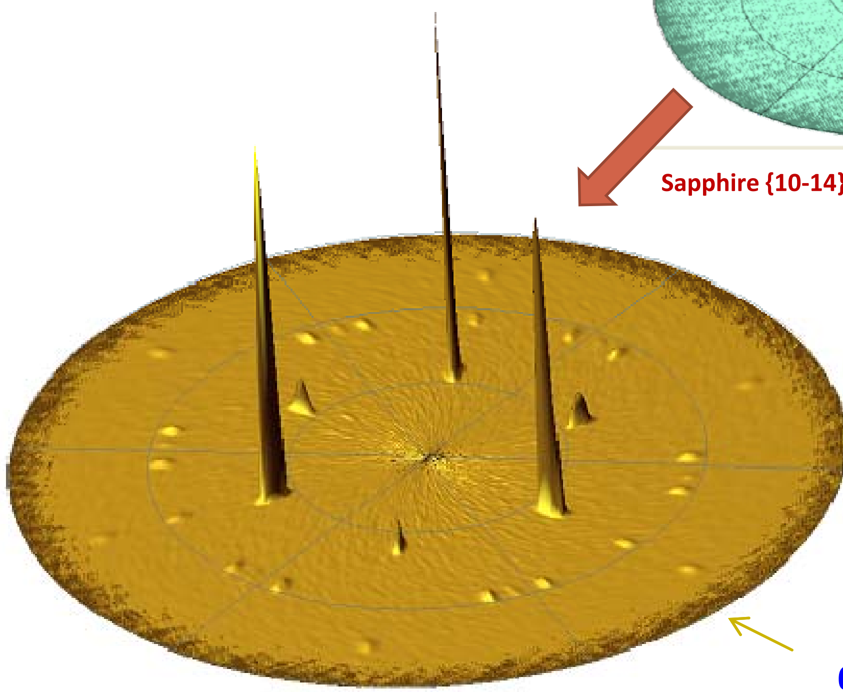

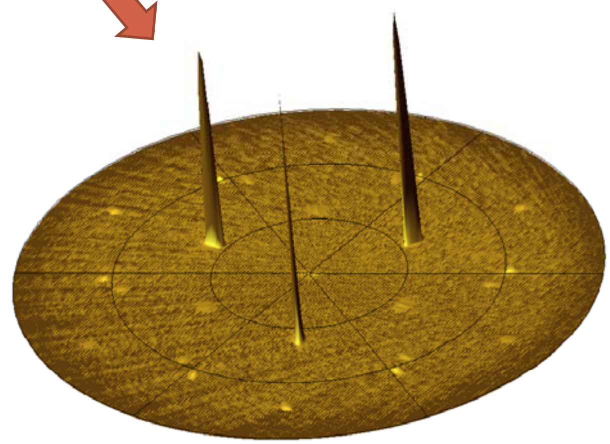

60 degree difference

SiGe {220}, Low Temperature

SiGe {220}, High Temperature

Wafer Mapping 1. (99.9999% single crystal)

Asymmetric angles for XY mapping with Point X-ray source

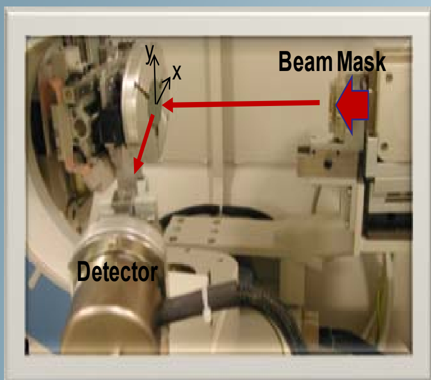

2Theta-Omega Normal Scan

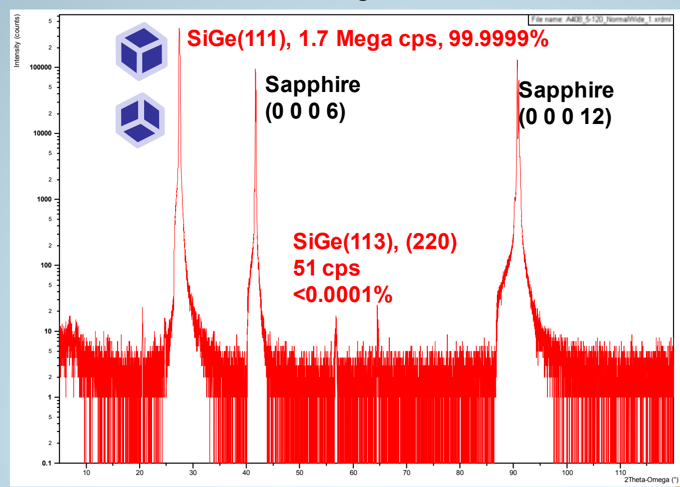

Point X-ray source for mapping

SiGe(440) Untilted Asymmetric Phi-Scan

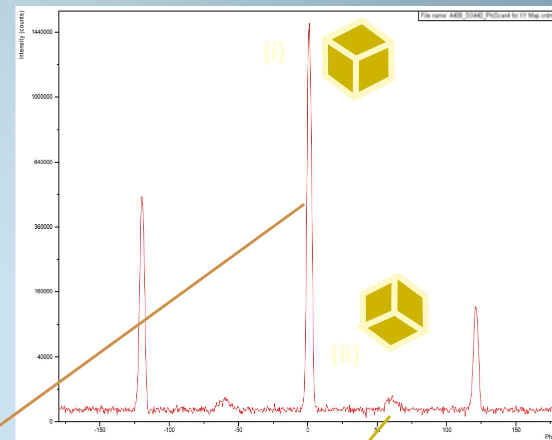

Wafer Mapping

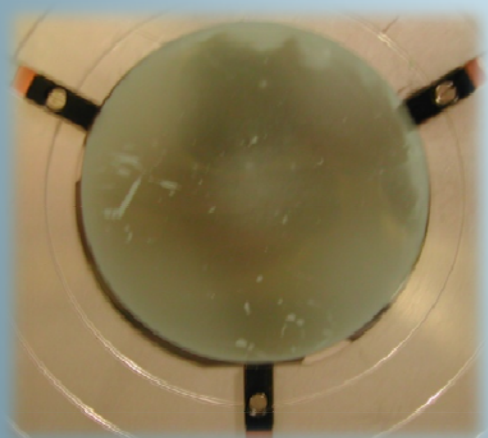

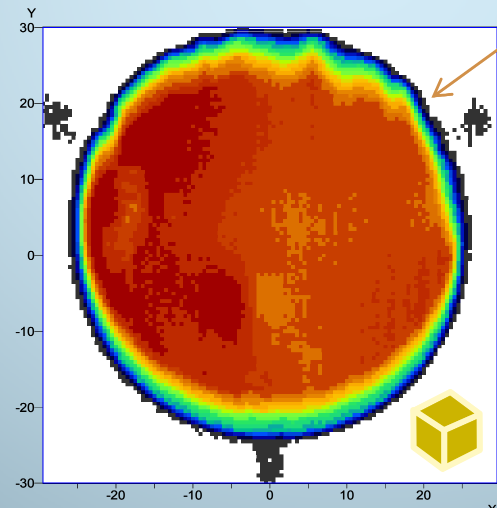

(i) Majority single crystal map

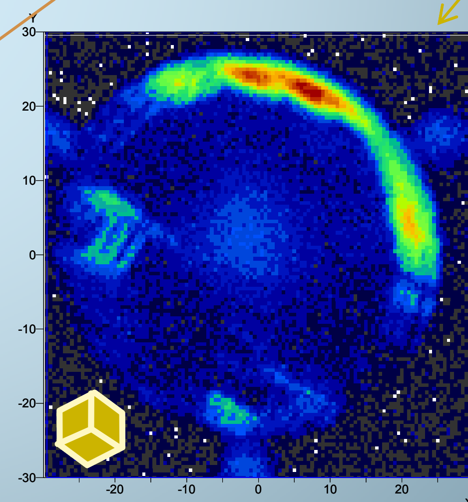

(ii) Defect map: Primary twin crystal rotated by 60° on (111) plane

Sample cage created + shaped thermal shadow

Power Sources for Spacecrafts

Fly-wheel Power Storage

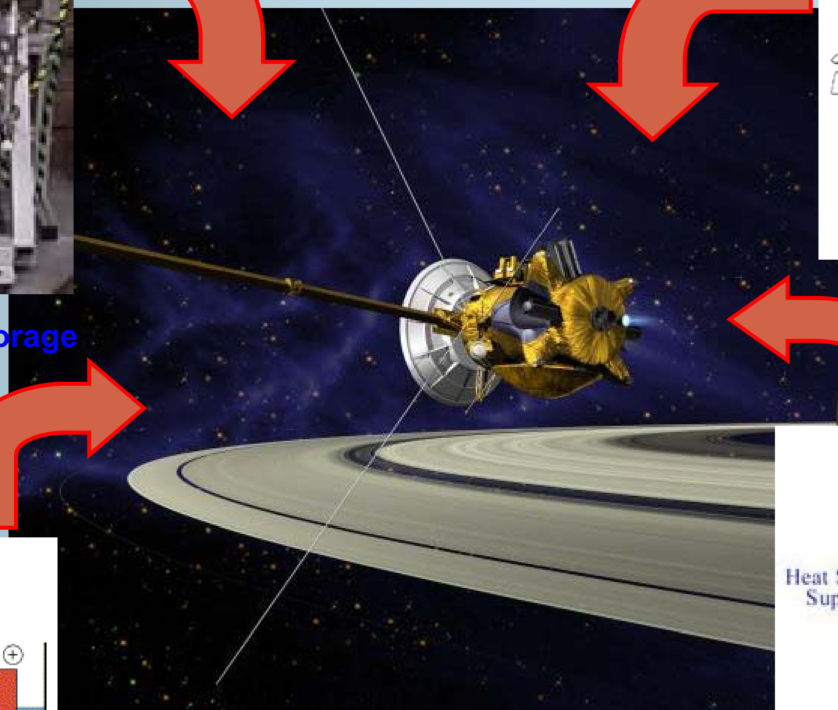

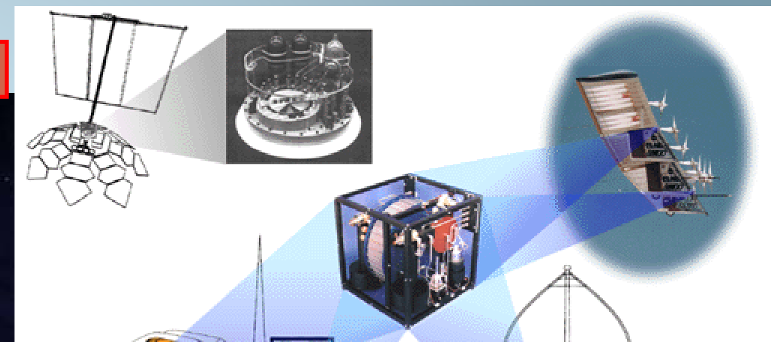

Fuel Cells

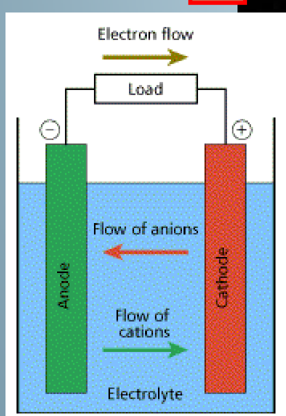

Canister-based Battery

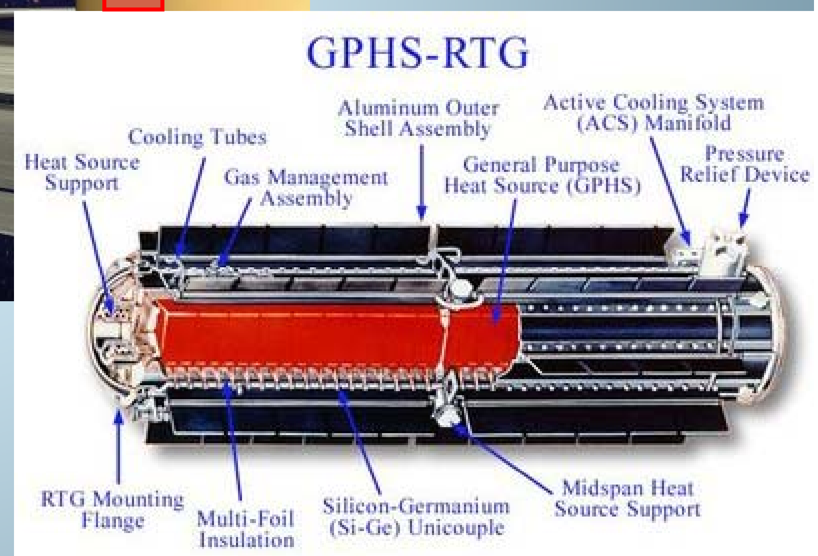

Radioisotope Thermoelectric Generators (RTG)

Advanced Thermoelectric Power Generation and Transmission System

The proposed system encompasses three subsystems:

1. Radioisotope Power (RIP) subsystem
2. Advanced Thermoelectric Generator (ATEG) subsystem
3. Wireless Power Transmission (WPT) subsystem

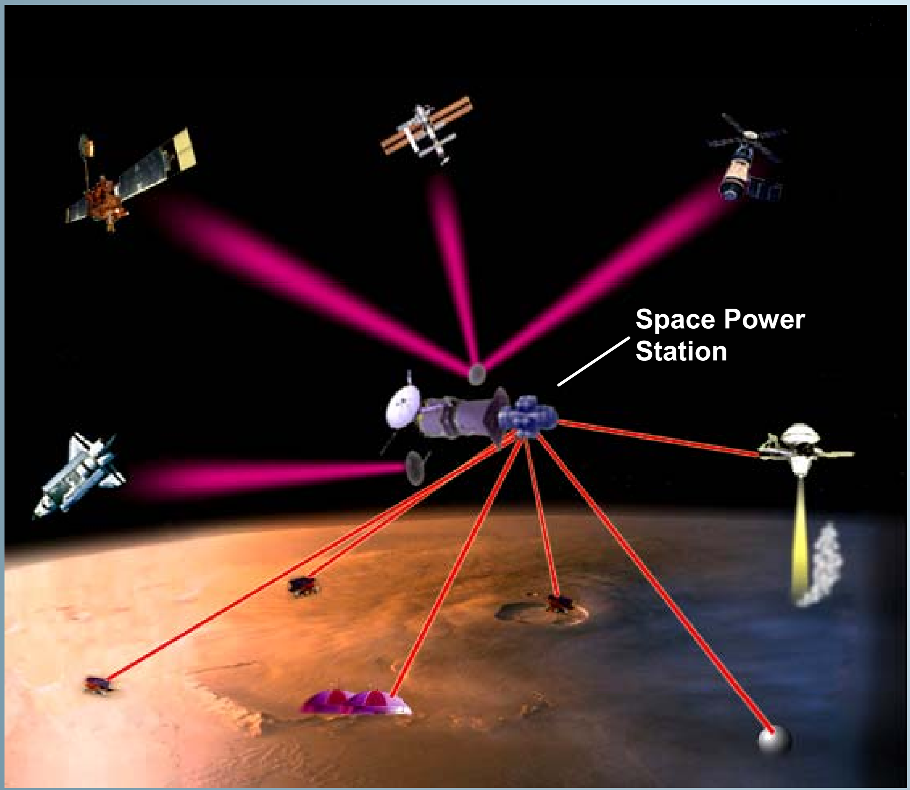

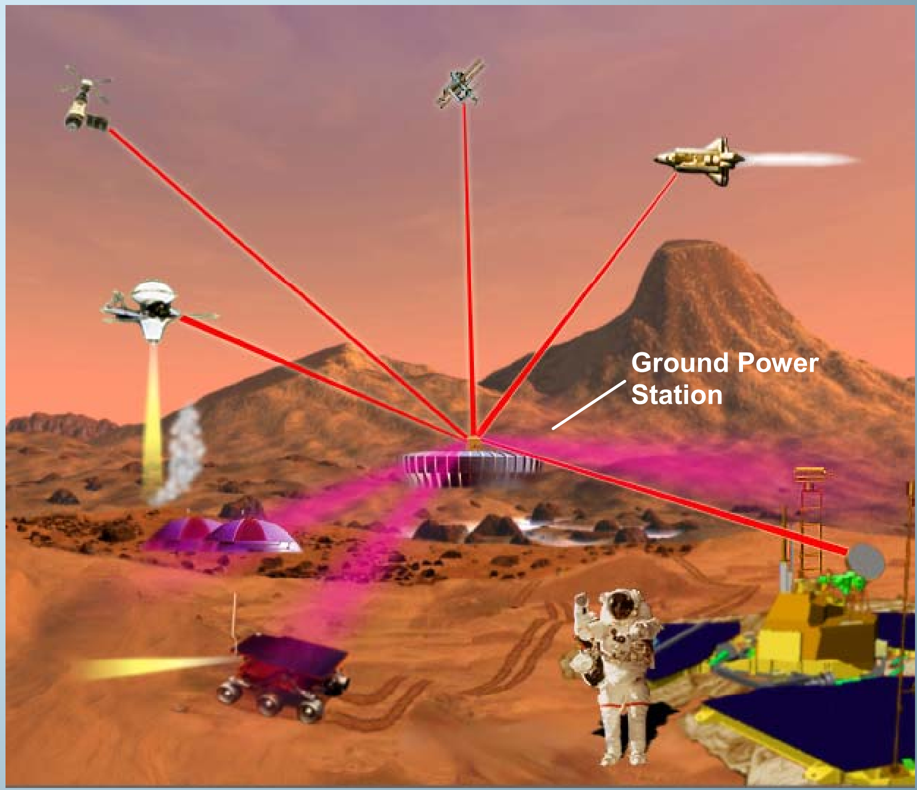

Artist's concepts of Mars space power station installed with WPT-ATEG system: space system (left) and ground system (right).

Solar Thermoelectrics: HAA Model with Ellipsoidal Cross-Section

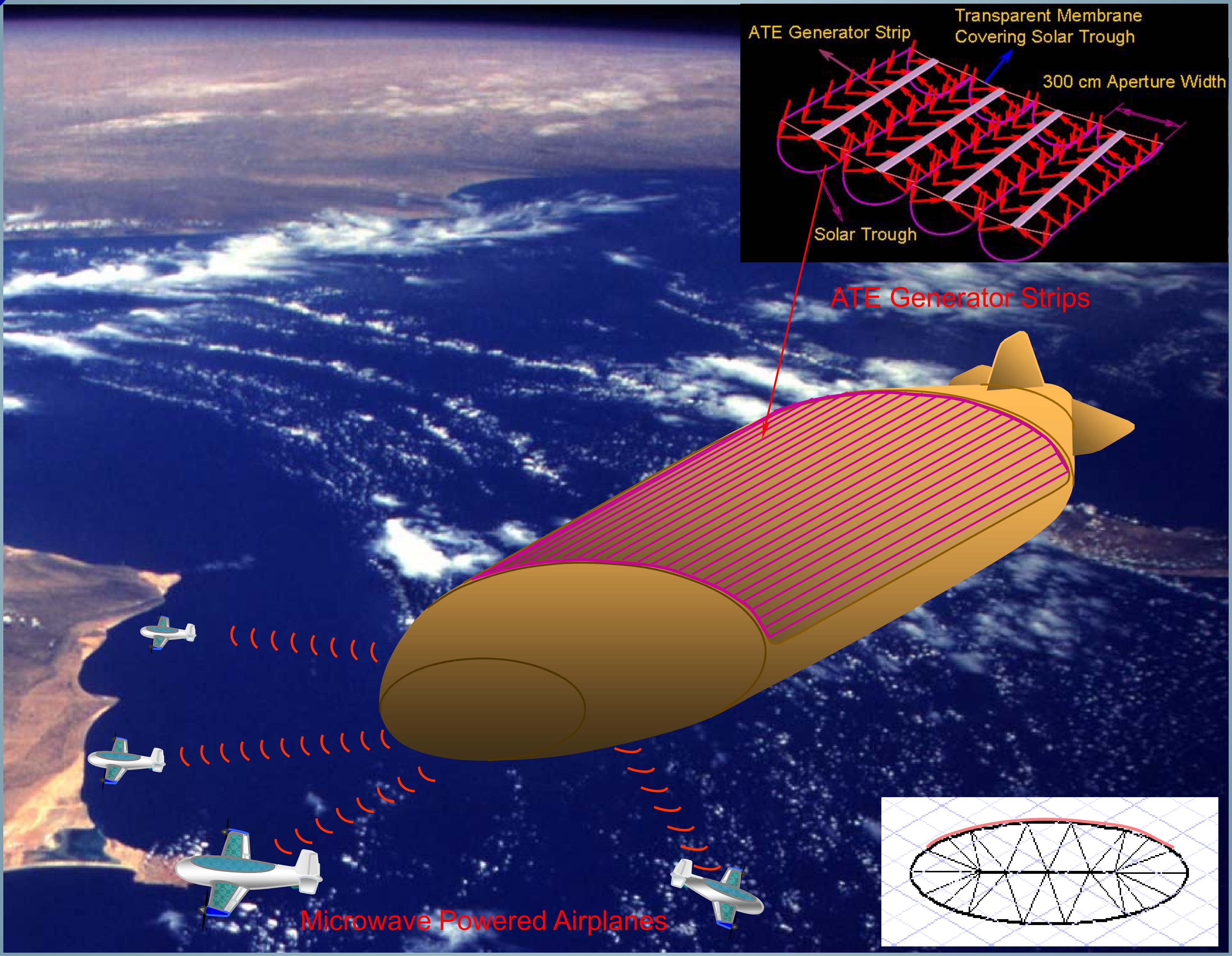

Distribution of Carriers and Ionization of Deep Levels

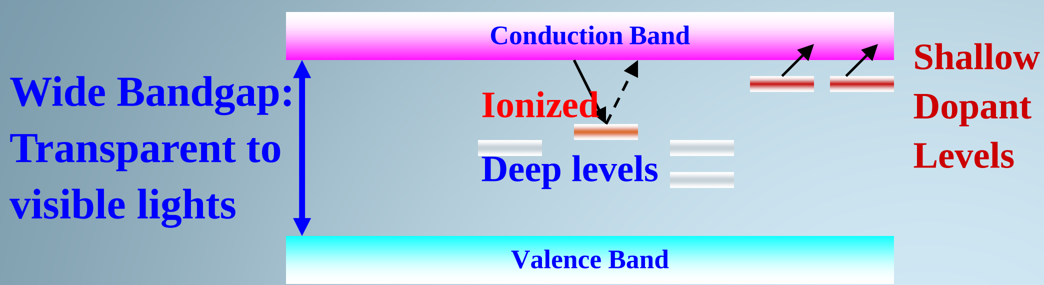

(1) Without Electric Field

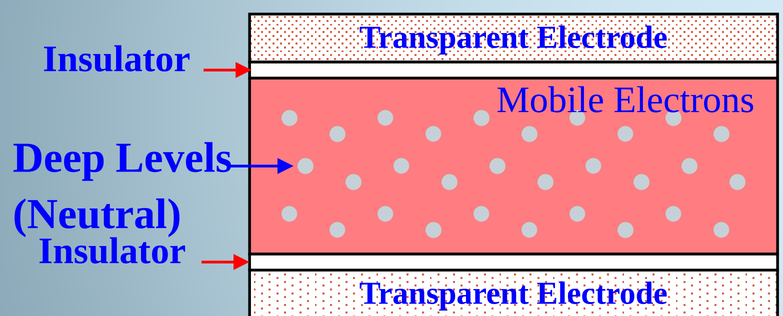

(2) With Electric Field: Redistribution of Mobile Electrons

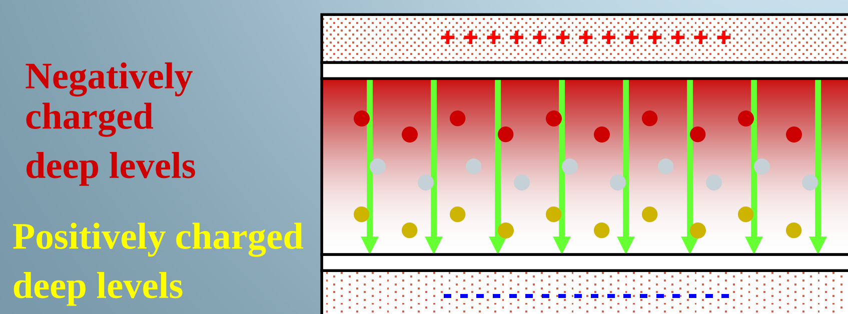

For wide band-gap materials:

- Transparent to visible lights
- Carriers in shallow dopant levels are mobile to conduction or valence band.
- Deep levels in crystal imperfection capture or emit mobile charges.
- Bandgap structure is ionized with the loss or capture of carriers.

For $|\bar{E}| = 0$,

- Mobile electrons distributed uniformly in media layer.
- Most of the deep levels are neutral in this state.

For $|\bar{E}| >> 0$,

- Mobile carriers (electrons in the picture) are re-distributed
- Deep levels are ionized and form new color centers.
- Absorption coefficient and index of refraction are changed

Hall Effect Measurement

As Grown ScN on Al_2O_3

Carrier Density: x10^4

● RESULTS

B =	0.51 [T]	D =	0.28 [um]
Nb =	-5.7963E+20 [/cm³]	Ns =	-1.6230E+16 [/cm²]
μ =	11.50203 [cm²/V·s]	Rh =	-1.0769E-02 [m³/C]
ρ =	9.3631E-04 [Ω·cm]	σ =	1.0680E+03 [1/Ω·cm]
delta_R =	1.9616E-02 [Ω]	alpha =	0.12167

Conductivity: x10^5

Nb : Bulk concentration
μ : Mobility
ρ : Bulk resistivity
delta_R : magnetoresistance
Ns : Sheet concentration
Rh : Hall coefficient
σ : Conductivity
alpha : V/H Ratio of Resistance

Intrinsic GaN on Al_2O_3

● RESULTS

B =	0.51 [T]	D =	0.397 [um]
Nb =	-6.6835E+16 [/cm³]	Ns =	-2.6534E+12 [/cm²]
μ =	2.22096 [cm²/V·s]	Rh =	-93.39652 [m³/C]
ρ =	52.87408 [Ω·cm]	σ =	1.8913E-02 [1/Ω·cm]
delta_R =	1.5208E+04 [Ω]	alpha =	0.16824

Nb : Bulk concentration
μ : Mobility
ρ : Bulk resistivity
delta_R : magnetoresistance
Ns : Sheet concentration
Rh : Hall coefficient
σ : Conductivity
alpha : V/H Ratio of Resistance

ScN grown on c-axis Sapphire (Al_2O_3) shows 10,000 times higher electron concentration than intrinsic GaN. This unintentional high-background- doping gives mobile charges in the media. With the applied electric field, the redistribution of mobile charges changes the index of refraction.

Change of the Index of Refraction in ScN

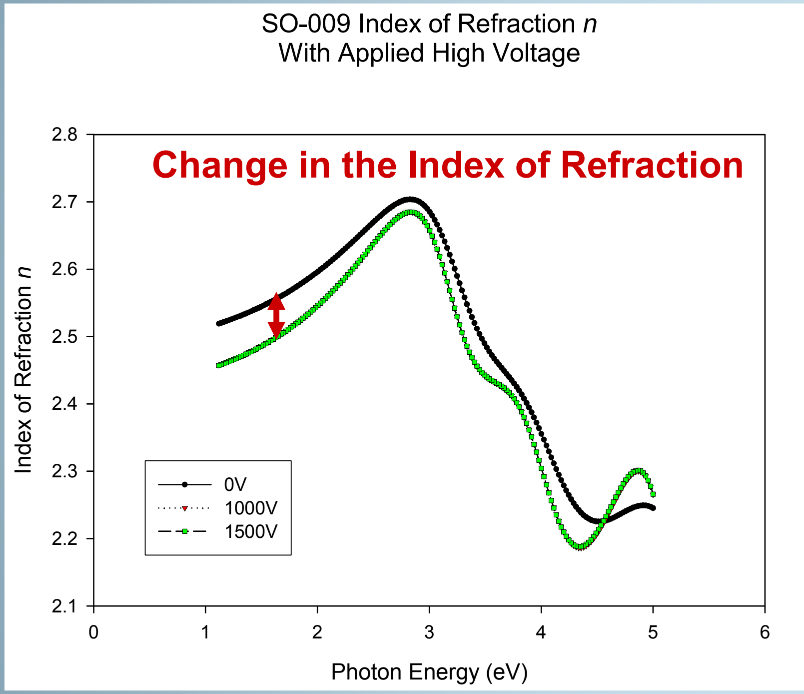

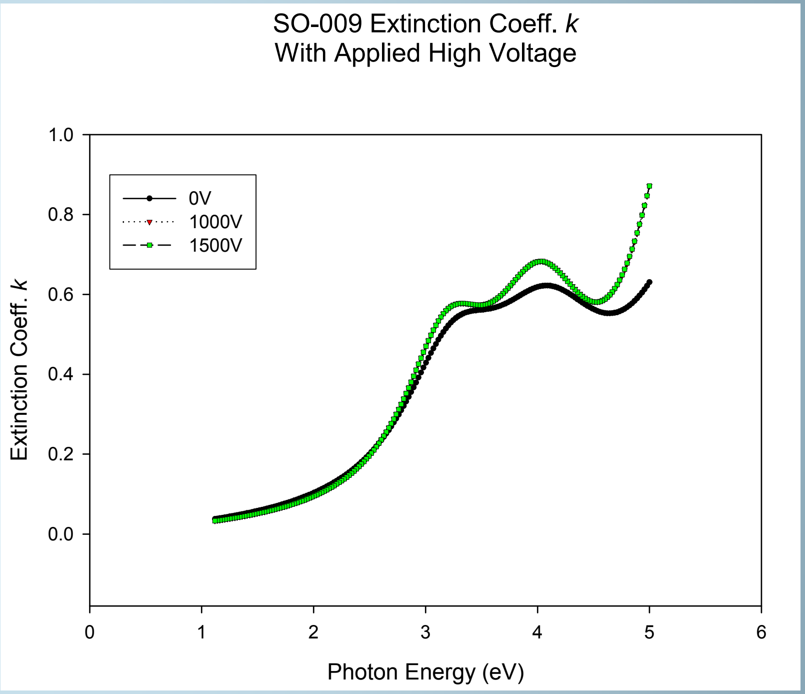

ScN film shows the change in the index of refraction with the applied electric field. The electric field was applied with a few mm gap. The required voltage can be reduced in the optimized structure.

$Ga_xSc_{1-x}N$ Alloy System

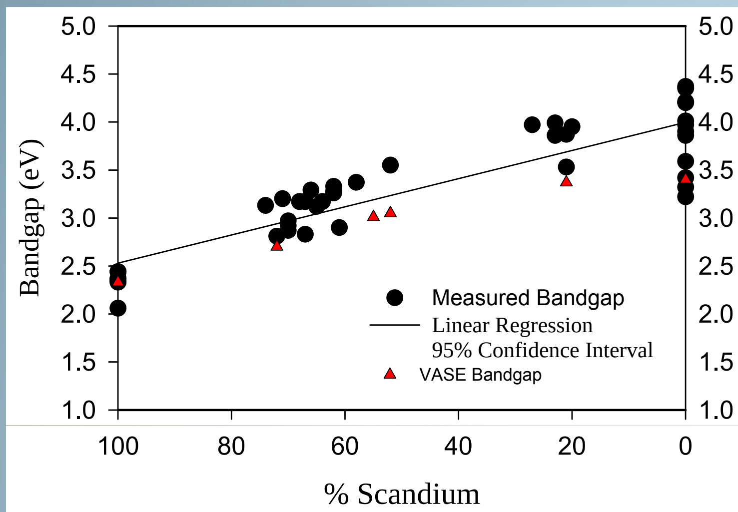

Bandgap Energy versus Scandium Concentration in $Ga_xSc_{1-x}N$ alloy system.

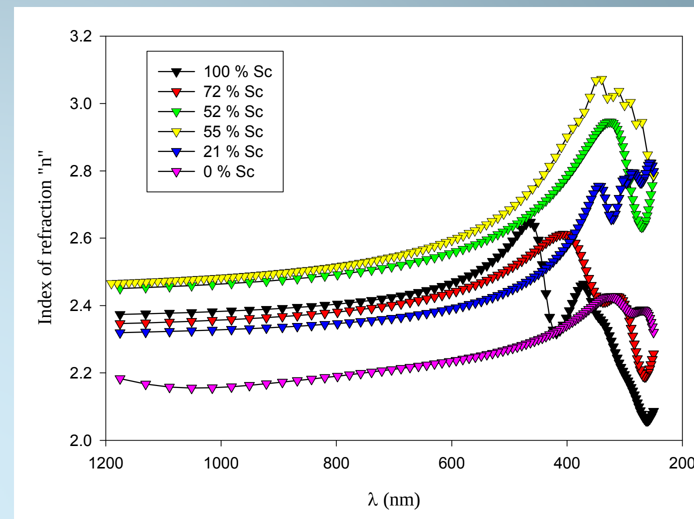

Index of refraction in the region below optical absorption

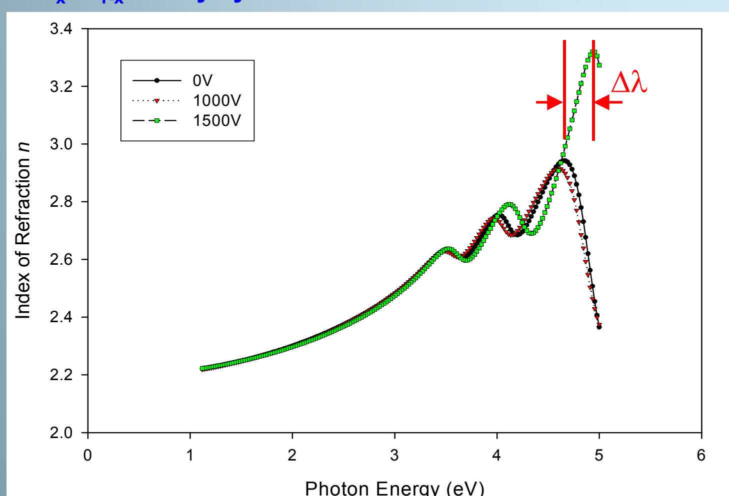

A thin-film of scandium-alloyed gallium nitride ($Ga_xSc_{1-x}N$, x=0.47) developed on a quartz substrate shows both the spectral and refractive index shifts very clearly from 3.5 eV to higher photon energy.

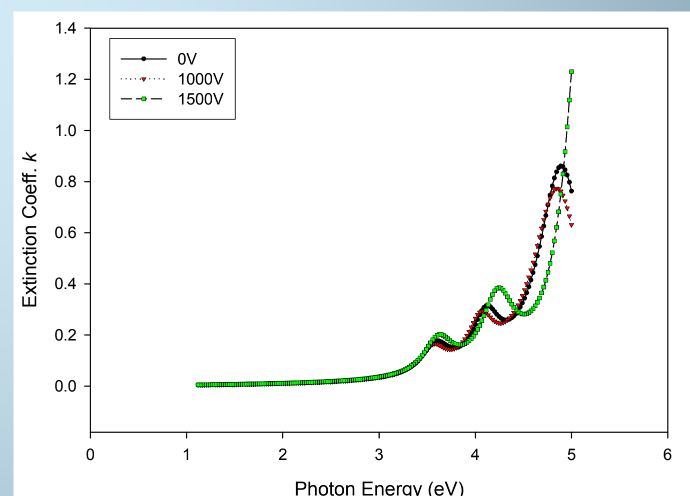

Extinction coefficient data shows a similar response as refractive index in the left, very clearly from 3.5 eV to higher photon energy.

Adaptive Optical Components

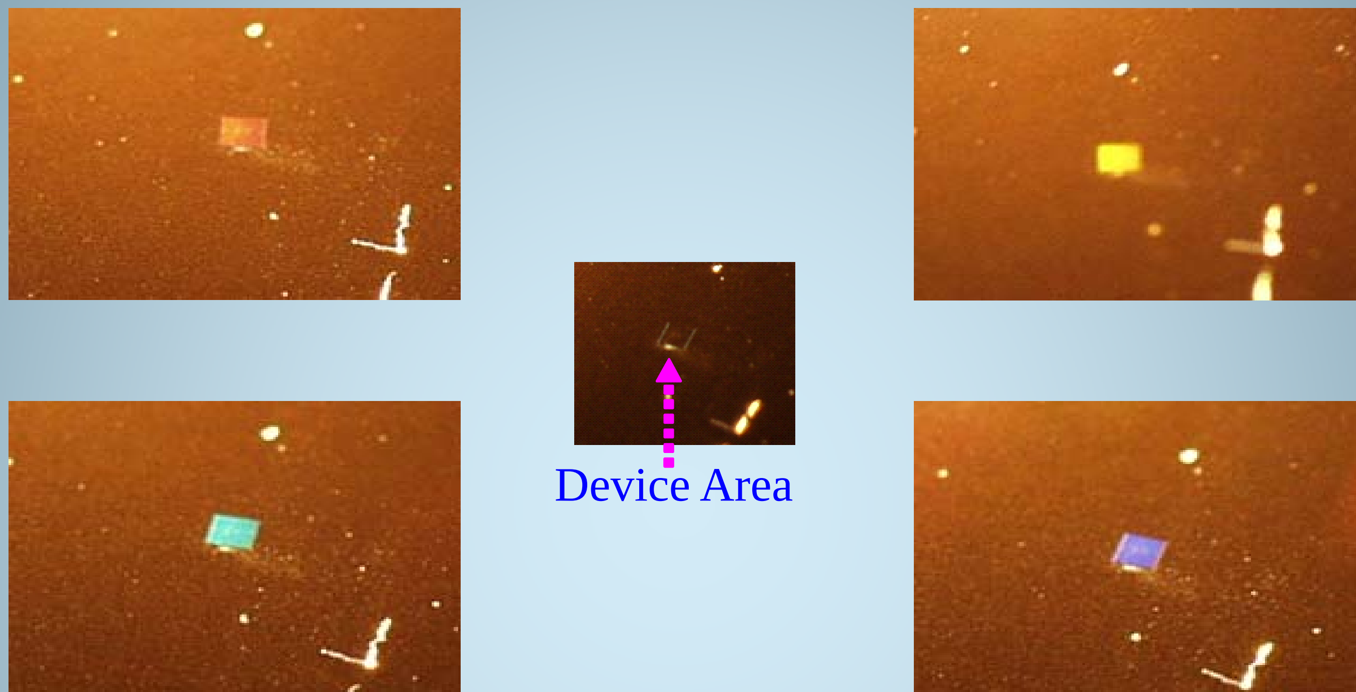

Geometric grating effect from the reflective array, fabricated at NASA LaRC

- The goal of Adaptive Optical Components: Adding a programmability to the conventional optical components, including lens, grating, apertures, filters and reflectors. The same optical component can be programmed for different wavelengths and polarizations.
- It can reduce the total weight of satellites and increase the working range and sensitivity of device with versatility.

Plasmon Enhanced Transmission

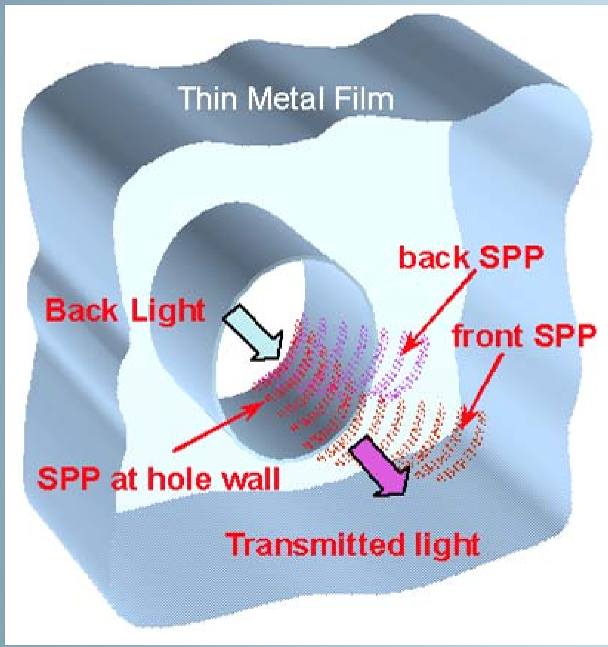

Transmission through a quantum aperture

- Metal surface has the collective movement of the electrons at the surface; it is called the surface plasmon, propagating on the surface only.
- The skin-depth of a good conductive metal is very shallow; a hundred nanometer metal film is enough to block the light penetration.
- The transmission of the photons through a hole smaller than 1/4 is controlled by the surface plasmons in the hole.
- The incident light generates the back surface plasmon. Surface plasmon propagates through the surface of the hole. On the front side, the surface plasmon radiates the light again.
- Other experiments indicate there is no enhanced transmission of a long wavelength light through tiny holes in Ge, where there is no plasmon. Only a good conductor surface has plasmon.

Nano Apertures

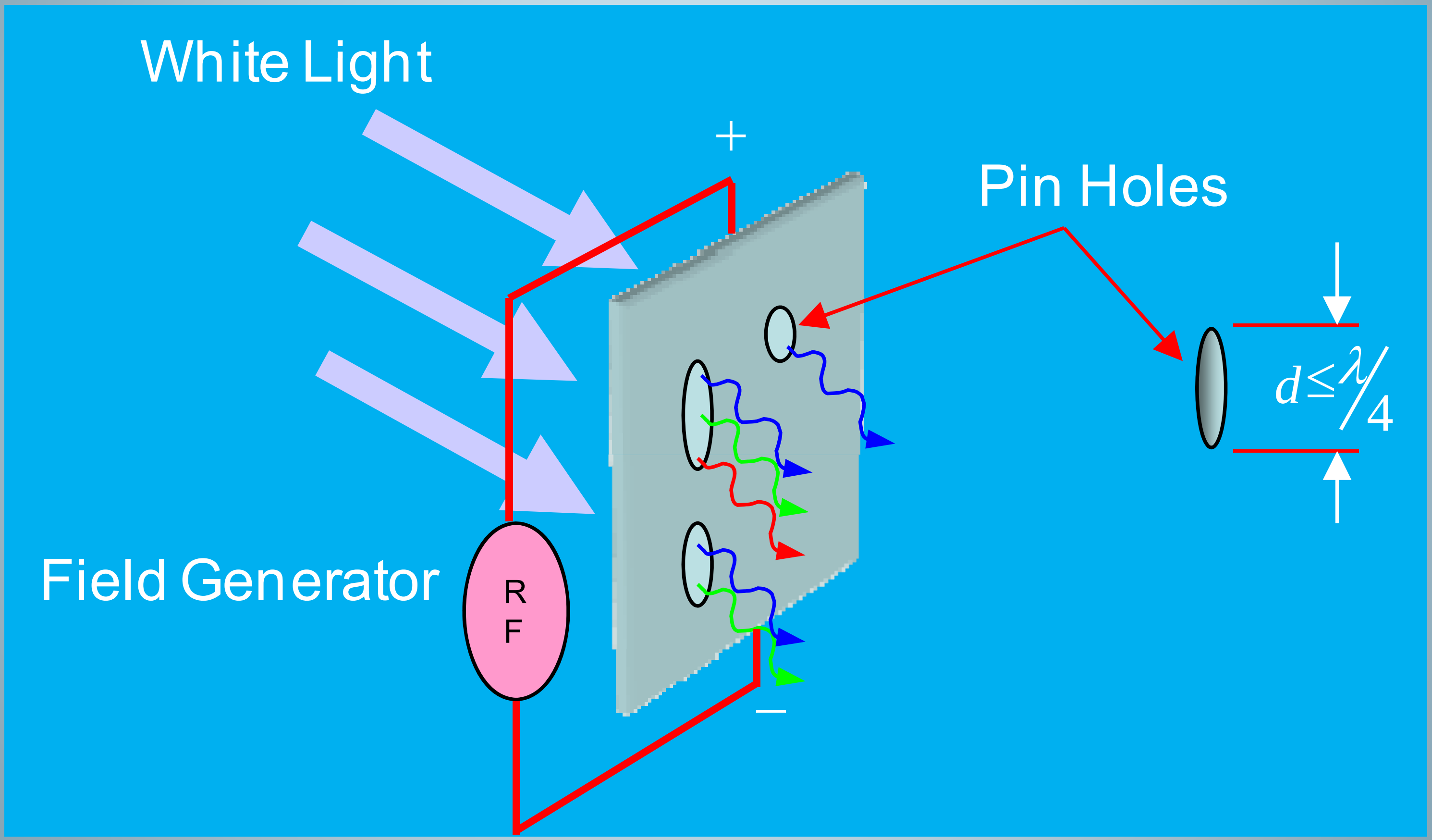

Microscopic Spectral Distribution From Individual Quantum Aperture with 200nm Diameter

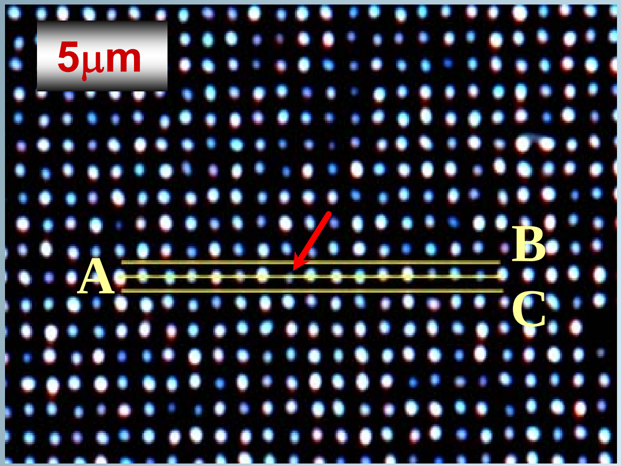

Transmitted Light

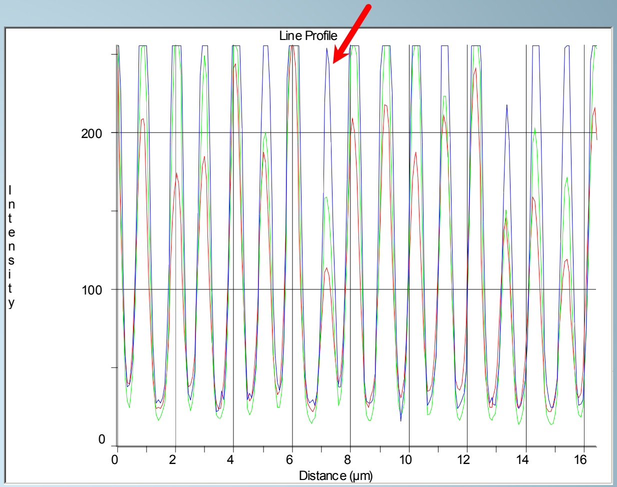

Center Line A: Strong Blue

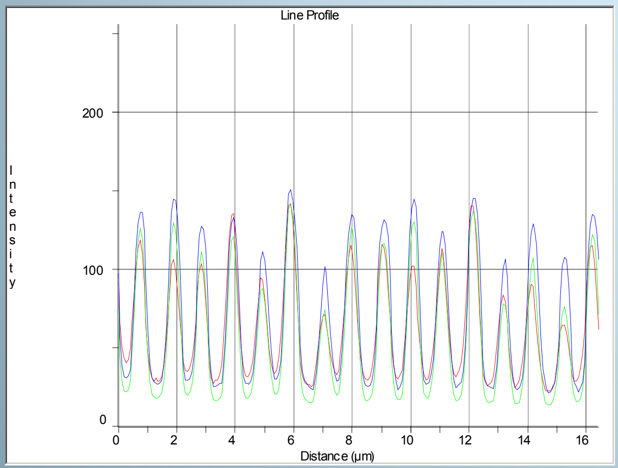

Sum of Area between B and C:
Close to White Light with Blue

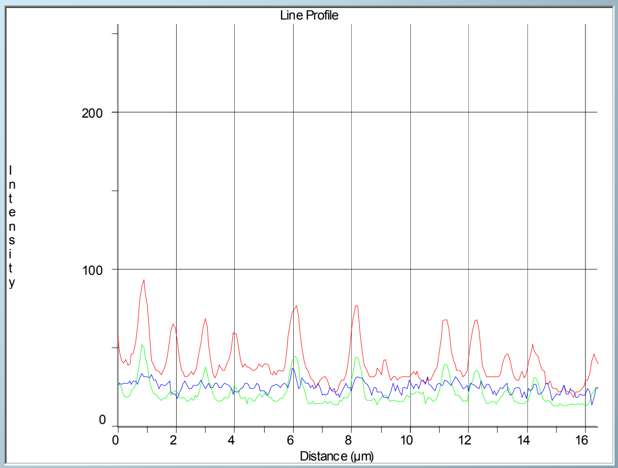

Boundary Line B or C:
Dark Red

Selected Light Transmission

Laser (532nm) + Front side illumination

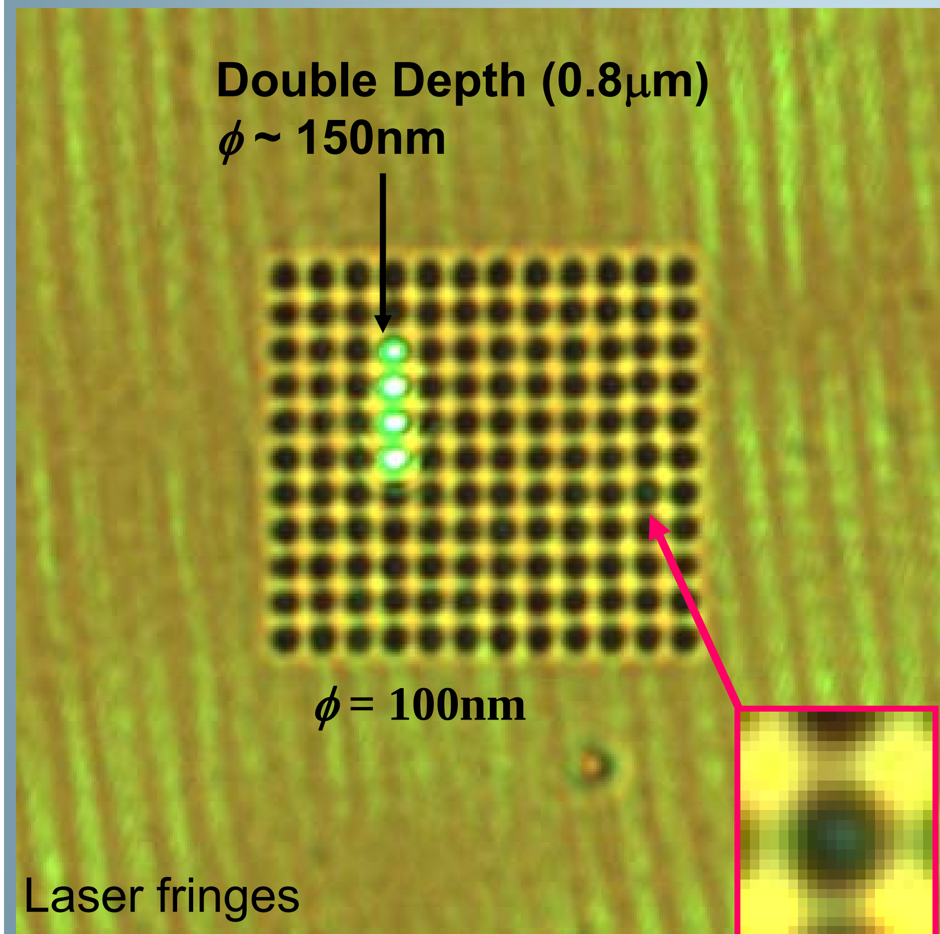

Laser (630nm) backside illumination only

Green light passes through.

Dual Sensing Capable Germ or Toxic Chemical (GTC) Sensor using Quantum Aperture Array with Surface Plasmon Polariton (SPP)

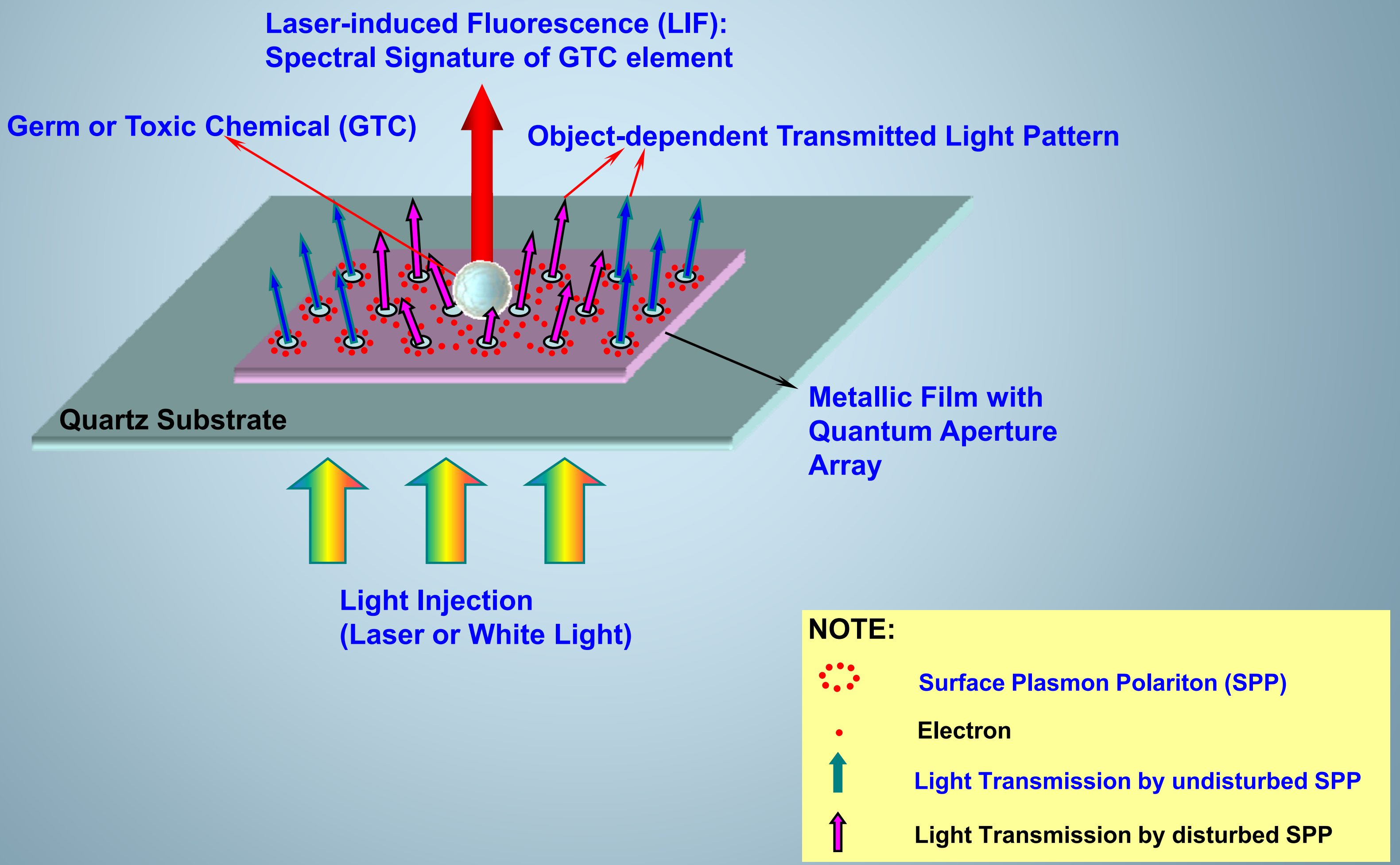

Micro Spectrometer (μ-SM) Applications

Medical Application for Neurosensing

Medical Sensors:
- Tiny form factor < 1 mm
- Flexible pin
- Sensor fusion capable
- Power & telemetry
- Redundancy feature

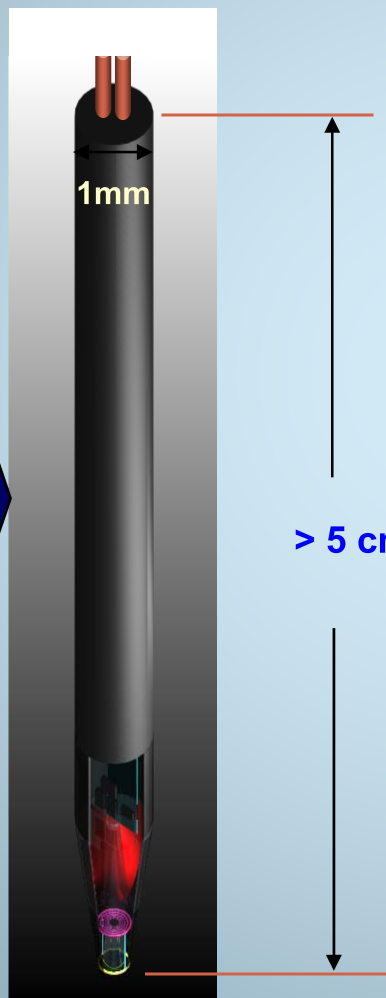

For Space Exploration

Leveraging Factors

Space:
- μ-SM imbedded rover tires
- μ-SM imbedded Astronaut's shoes
- μ-SM imbedded canes or darts
- Hyperspectral imaging

Aeronautics:
- Engine combustion monitoring
- Fuel leak detection
- Hyperspectral Lidar imaging

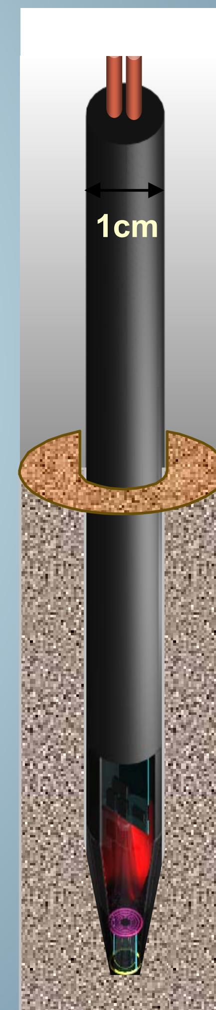

Can be used in
Tumble-weed type
planetary surface explorer

Sharpness of focal point P1 and PX with a green laser (λ=532nm)

10 mW Laser in 2mm diameter (0.3 W/cm^2) can have a focused power density = 10^5 Watt/cm^2

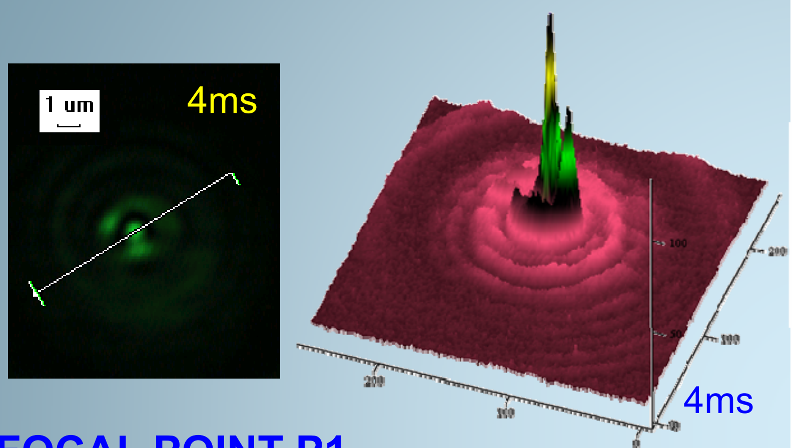

FOCAL POINT P1

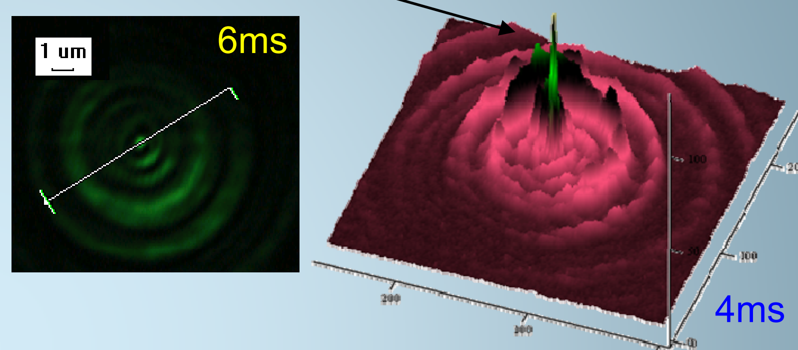

FOCAL POINT PX

(2μm before destructive interference height)

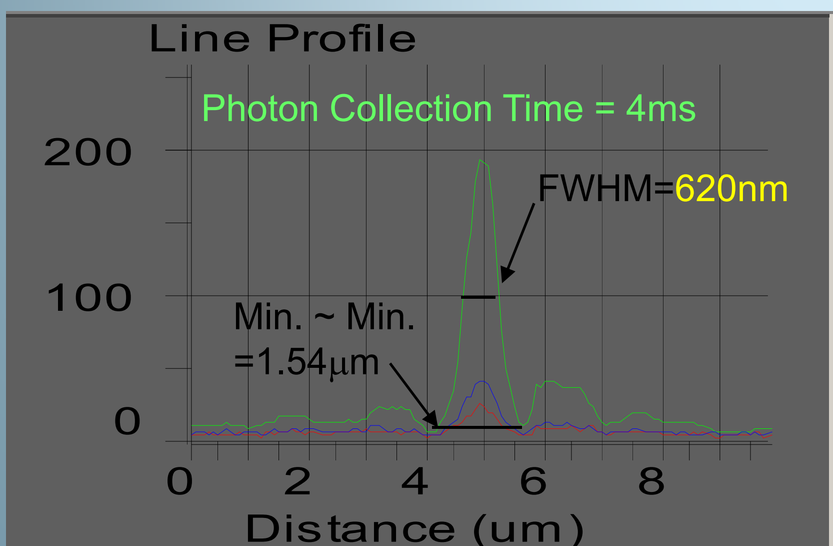

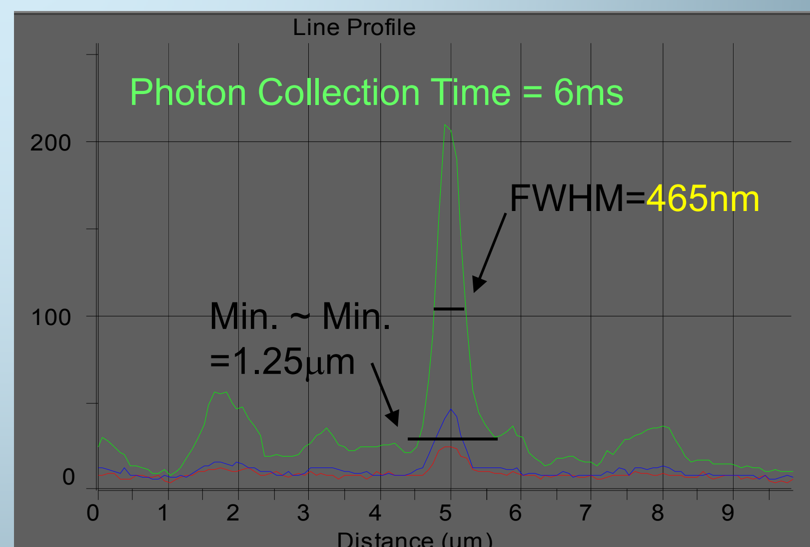

Photonic DART Technology

(**D**ensely **A**ccumulated **R**ay-point by micro-zone-pla**T**e)

Spectral scans:

Circular Grating: 100 rings, 750μm diameter
Aperture: 10 μm diameter

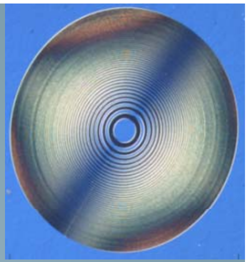

Green Laser: 532nm

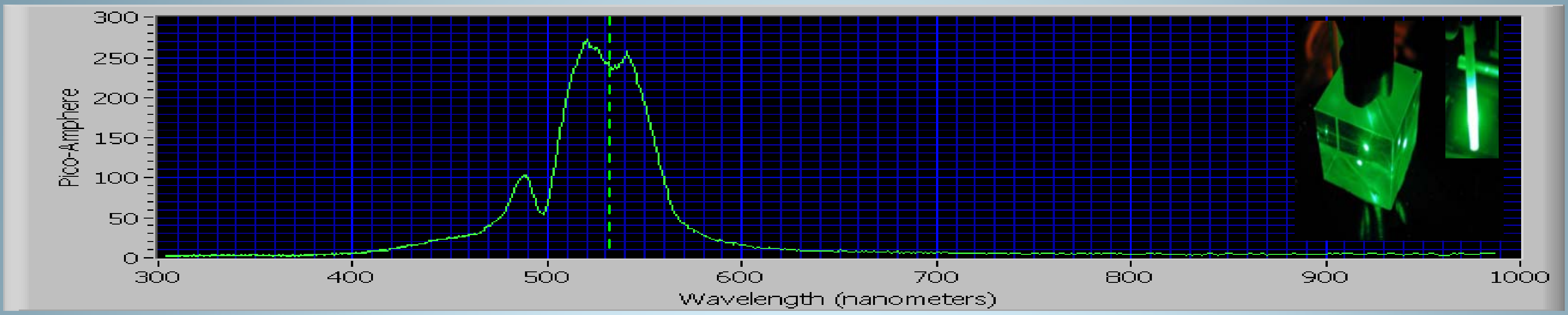

Red Laser: 633nm

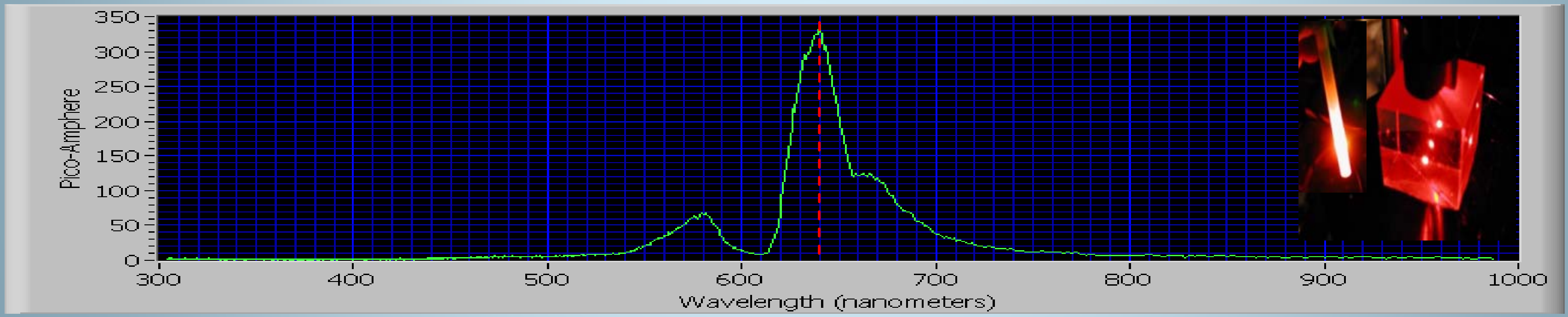

Green & Red Lasers: 532nm & 633nm

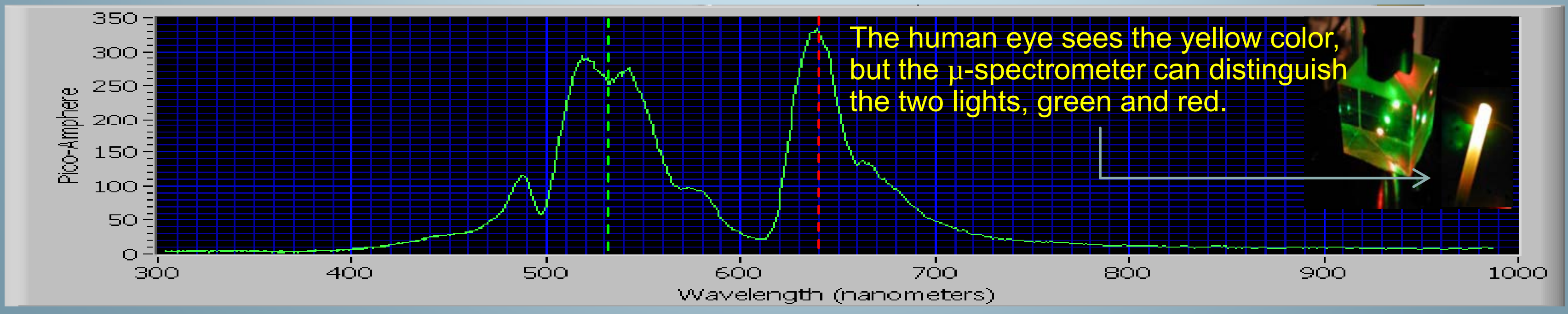

μ-Spectrometer (μ-SM) Applications
Lunar & Mars Exploration

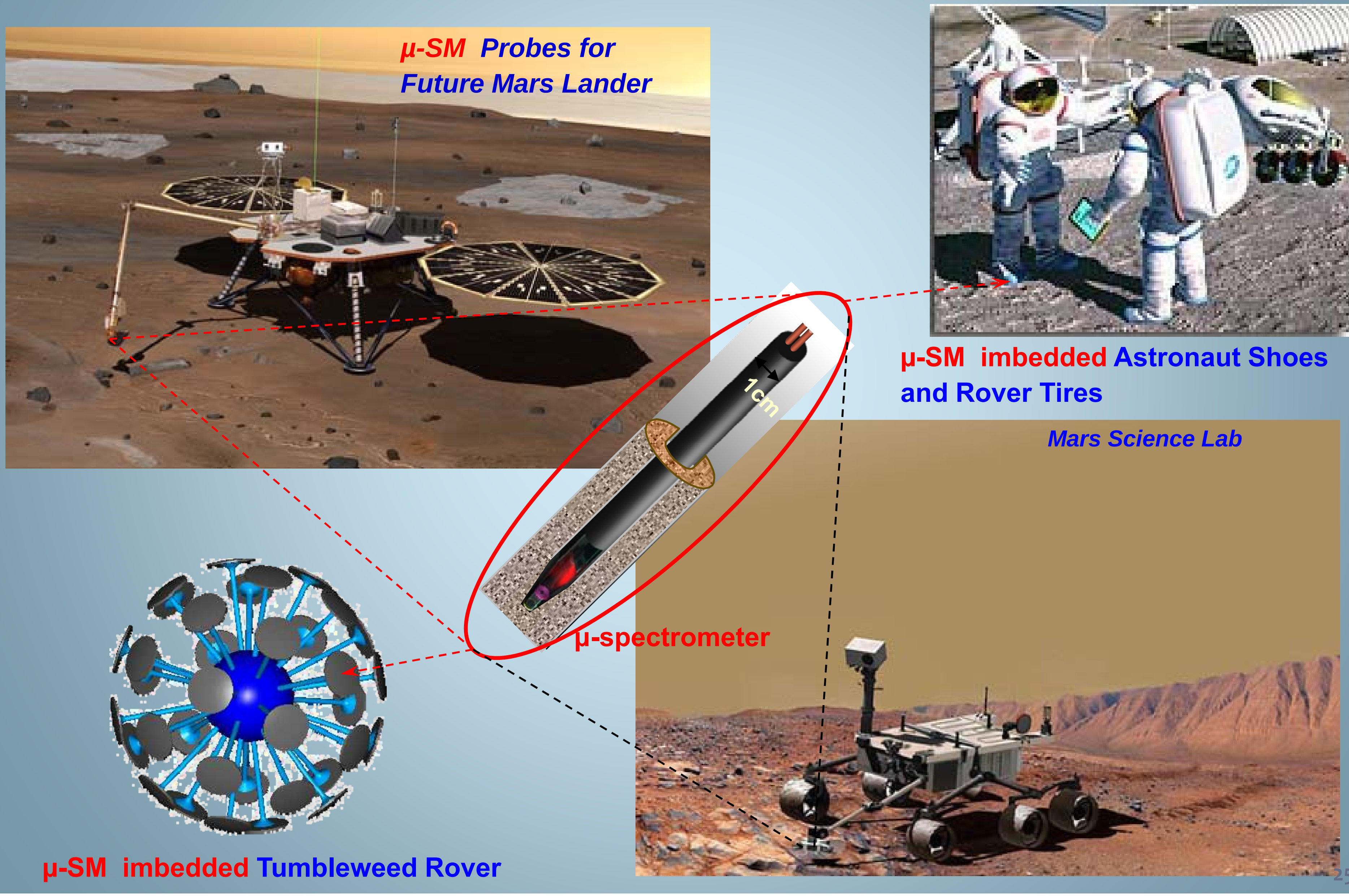

Aero-Space Application

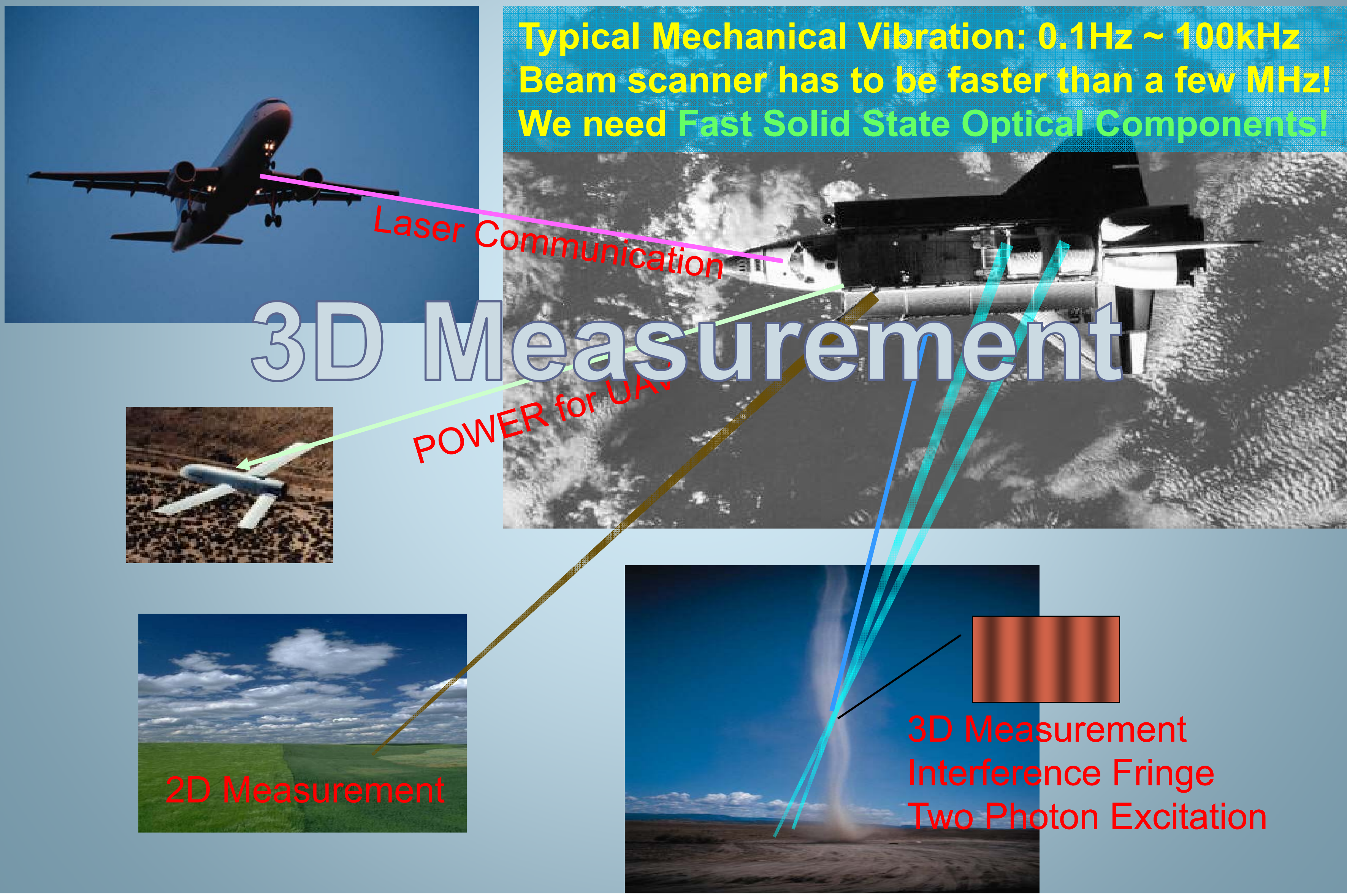

Lithography and Etched Patterns

E-Beam Lithography

Single Beam Scanner

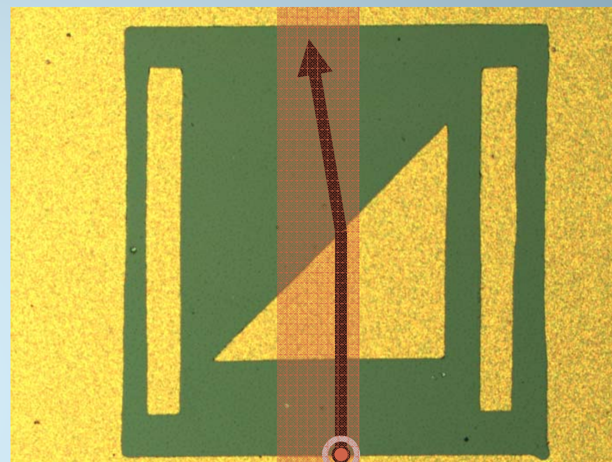

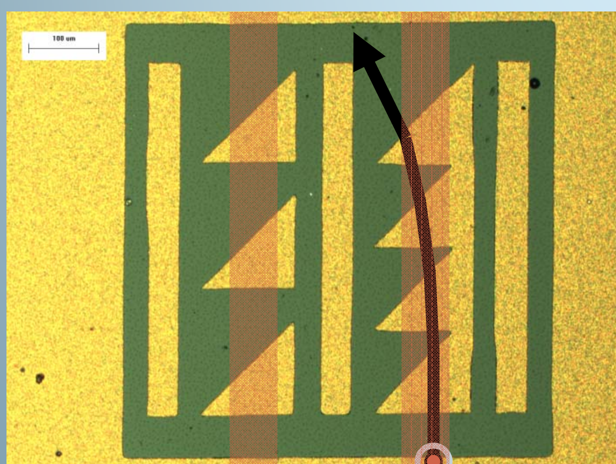

Beam Scanner Array

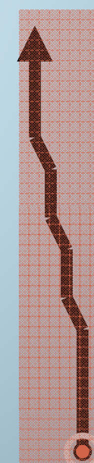

Beam Displacer

Light Control Device

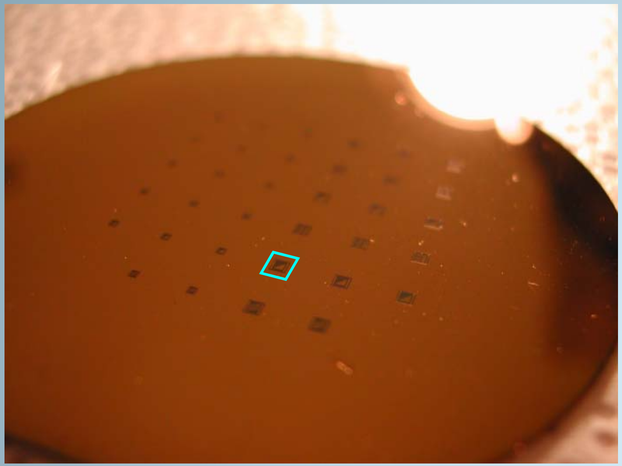

Patterns made with E-Beam Lithography

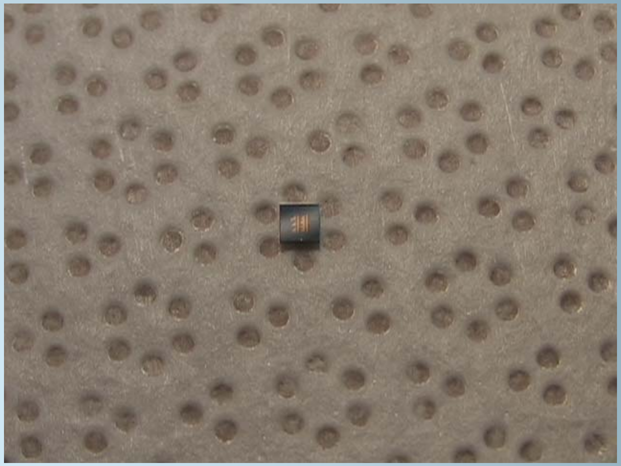

All-Solid-State Beam Scanner

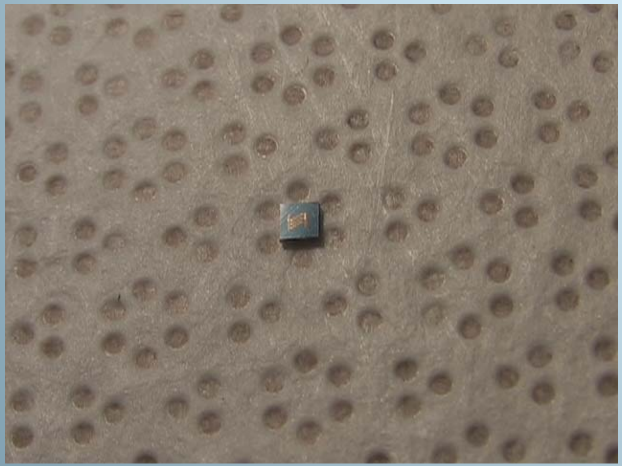

All S.S. Beam Scanner Array

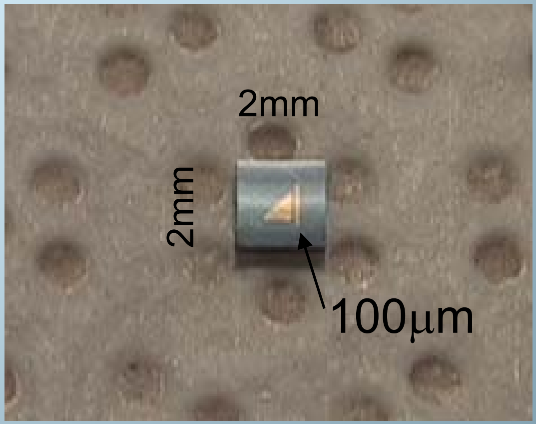

Solid State Beam Displacer

Ferritin Protein

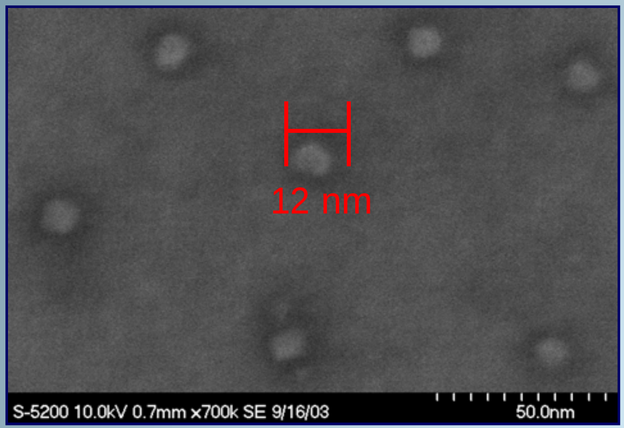

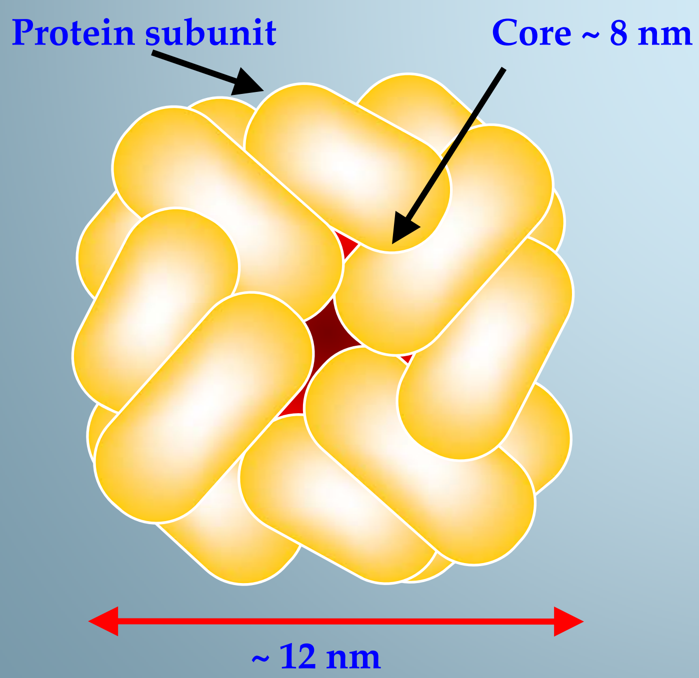

- Iron storage protein in biological mechanisms in human, animal, and even bacteria
- 24 subunits
- Contains up to ~4500 Fe^{3+} atoms
- Stable and robust structure to withstand biologically extremes of high temperature (up to 80 °C) and pH variations (2.0-10.0)
- 2, 3, 4-fold symmetry channels for the transport of ions and molecules.
- Hydrophilic 3 fold (Fe^{2+})/ Hydrophobic 4 fold
- Electron conduction through ferritin shell is possible.
- Core materials –
  - Iron (Fe), Cobalt (Co), Manganese (Mn),
  - Nickel (Ni), Platinum (Pt),
  - Semiconductors (CdS, CdSe)
  - Magnetite-maghemite
  - Trimethylamine-N-oxide, etc.

Biomineralization & Reconstitution of Ferritin Core

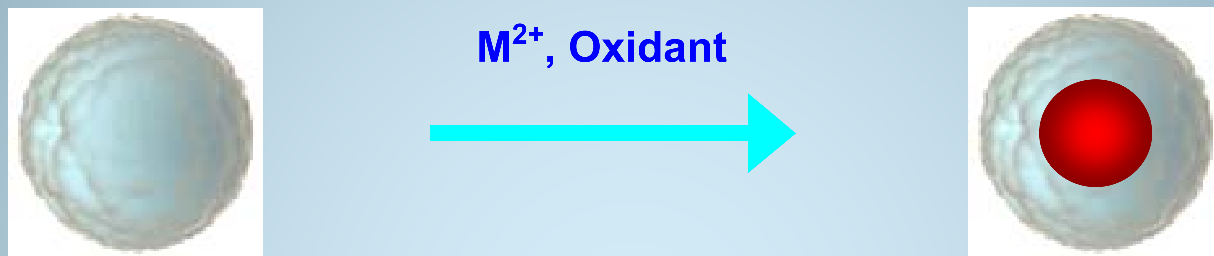

Apoferritin

Ferritin reconstituted with M^{3+}

$$4\,M^{2+}_{(aq)} + O_2 \rightarrow 4\,M(O)OH_{(s)} + 8\,H^{+} + 2\,H_2O$$

M : Core materials ---- Fe (natural)

Co, Mn, Ni, Pt, As, P, V (successful)

CdS, CdSe (successful)

Magnetite-maghemite (ferrimagnetic)

Trimethylamine-N-oxide (superparamagnetic)

Chemically Reconstituted Ferritins

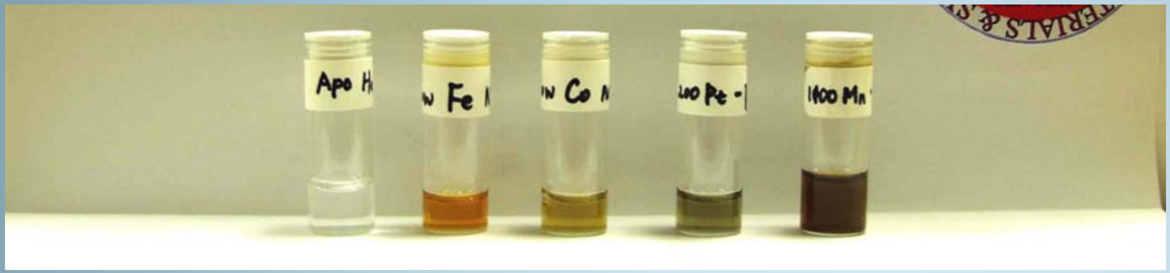

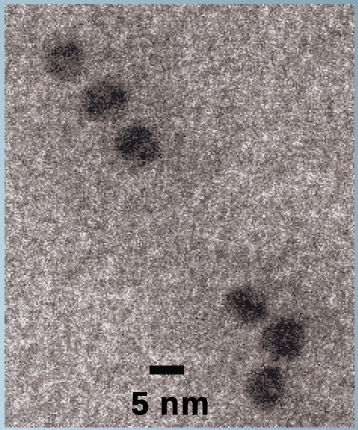

STEM image of Fe-cored ferritins

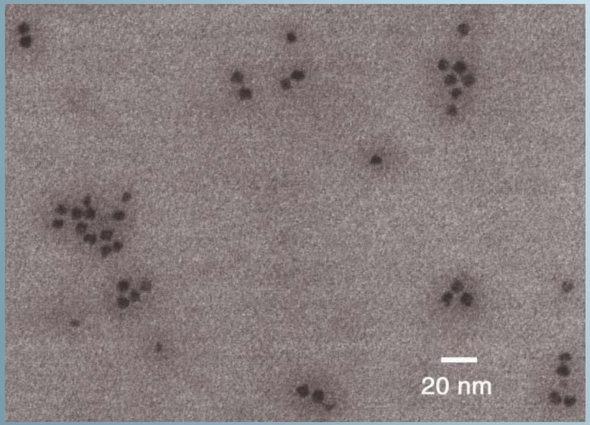

Fe-cored ferritins

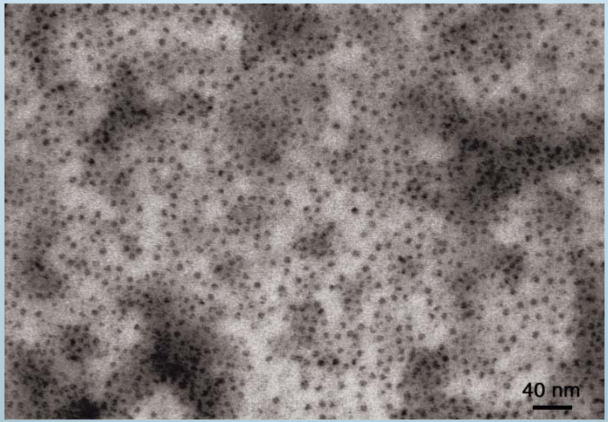

Co-cored ferritins

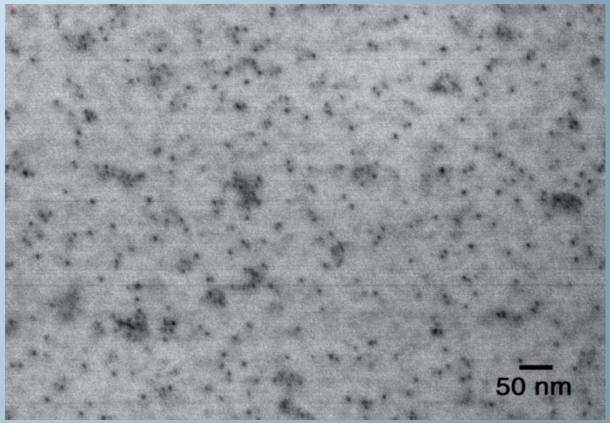

Mn-cored ferritins

Inorg. Chem., **44**, 3738-3745 (2005).
Chem. Commun., (32), 4101 -4103 (2005).

Why Bio-Nanobattery ?

What about

- **Distributed** power storage ?
- **Flexible thin-film** battery ? - Designer's dream !!
- **Easy embodiment** with power harvesting devices ?
- **Biocompatibility** with in-vivo nanodevices ?
- **Light weight** and high energy density ?
- **Chip scale power source ?**
  - Intelligent and autonomous operation

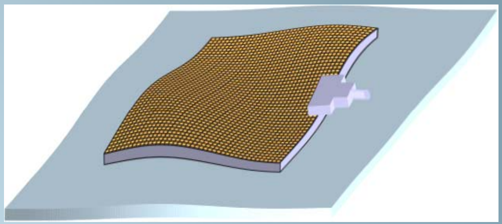

Flexible Nanobattery Film

Wearable Electronics (Philips)

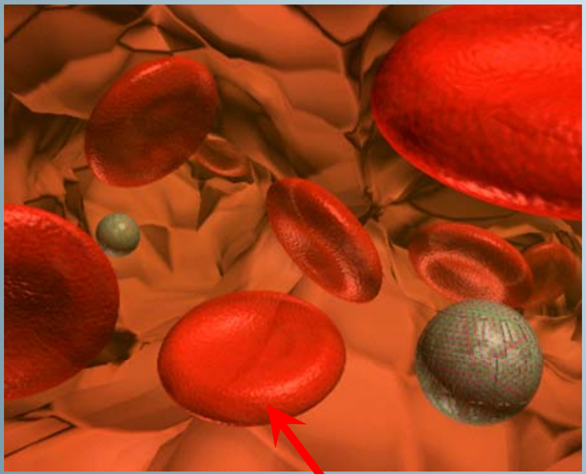

Red Blood Cell

Bio-nanobattery patch installed in autonomous bio-nanorobot

Bionanobattery Concept

Fe^{2+}- ferritin **Co^{3+}-ferritin**

$$Fe(OH)_3 + e^- \leftrightarrow Fe(OH)_2 + OH^- \qquad E^o = -0.49V$$

$Fe(OH)_3/Fe(OH)_2$ II $CoOOH/Co(OH)_2$ $E_{cell} = 0.66$ V

$Fe(OH)_3/Fe(OH)_2$ II γ-$MnOOH/Mn(OH)_2$ $E_{cell} = 0.20$ V

$Fe(OH)_3/Fe(OH)_2$ II $NiOOH/Ni(OH)_2$ $E_{cell} = 0.97$ V

Theoretical Values of Bionanobattery

→ Anode

↓ Cathode

	Zn	Cd	Fe	V	Hg	Mn	Co	Ni
Zn								
Cd	0.422							
Fe	0.756	0.334						
V	0.760	0.338	0.004					
Hg	1.344	0.922	0.588	0.584		0.388		
Mn	0.956 (1.606)*	0.534 (1.184)	0.200 (0.850)	0.196 (0.846)	(0.262)		(0.190)	
Co	1.416V	0.994	0.660	0.656	0.072	0.120		
Ni	1.726	1.304	0.970	0.966	0.382	0.770	0.310	

Zn^0/Zn^{2+}: -1.246 V

Cd^0/Cd^{2+}: -0.824 V

Fe^{2+}/Fe^{3+}: -0.49 V

V^{2+}/V^{3+}: -0.486 V

Hg^0/Hg^{2+}: 0.098 V

Mn^{2+}/Mn^{3+}: -0.29 V

Co^{2+}/Co^{3+}: 0.17 V

Ni^{2+}/Ni^{3+}: 0.48 V

()* Mn represents as γ-MnO_2 inside Ferritin.

Ni-Cored Ferritin

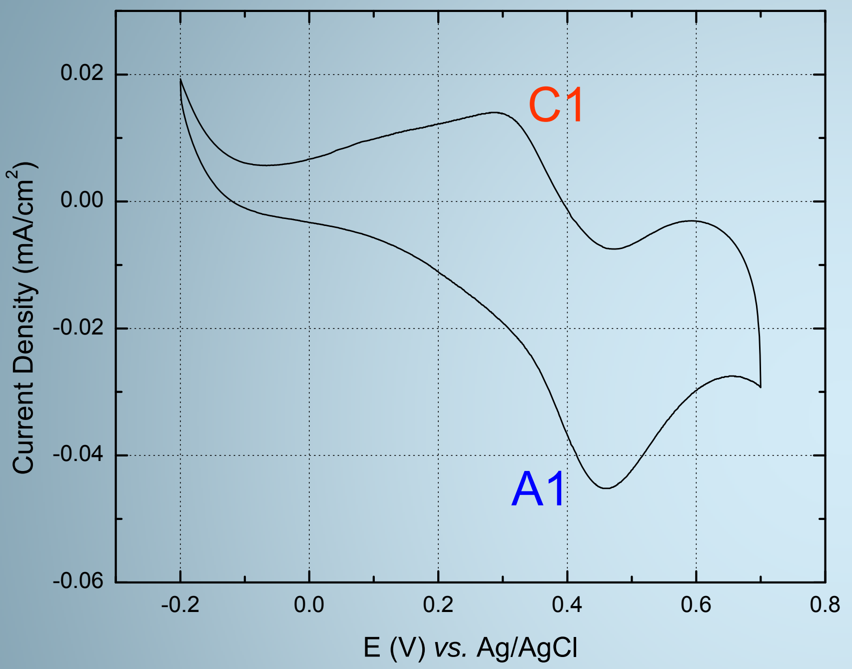

C1: $NiOOH + H^+ + e^- \rightarrow Ni(OH)_2$

A1: $Ni(OH)_2 \rightarrow NiOOH + H^+ + e^-$

CV of physically adsorbed Ni-cored ferritin on Au electrode in 0.05 M phosphate buffer (pH 7.5 and pH 9.0) at the scan rate of 100 mV/s.

	Co	Mn	Ni
Fe	500 mV	480 mV	790 mV

Fe-Co Bionanobattery Cell – Wet Cell

Bionanobattery Demo Cell

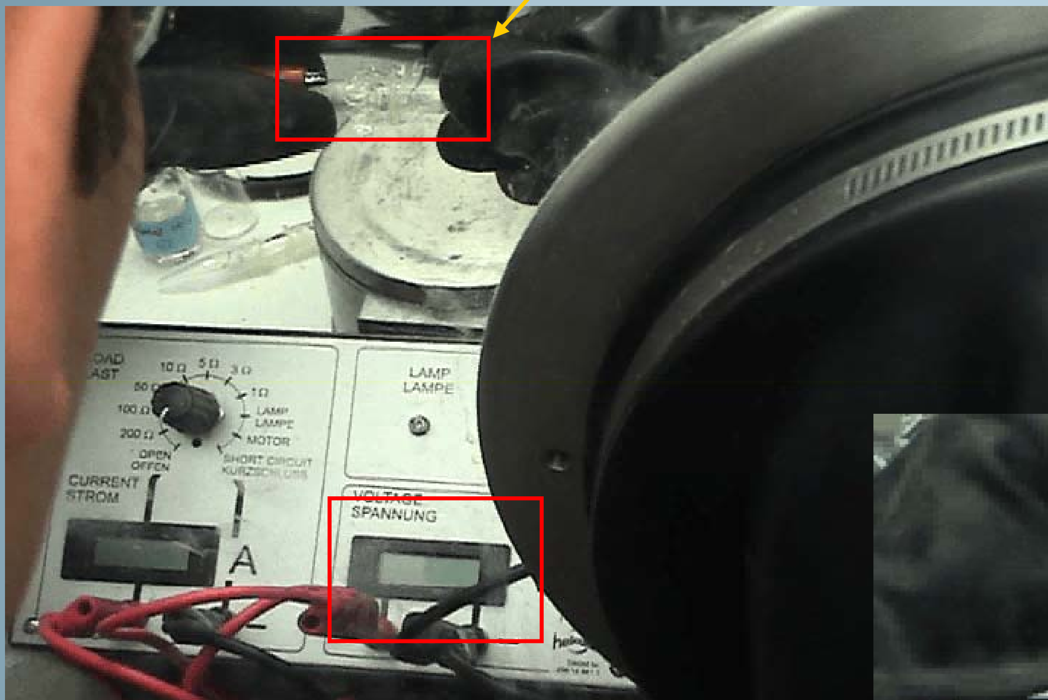

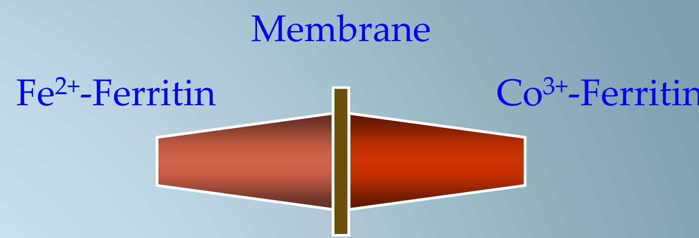

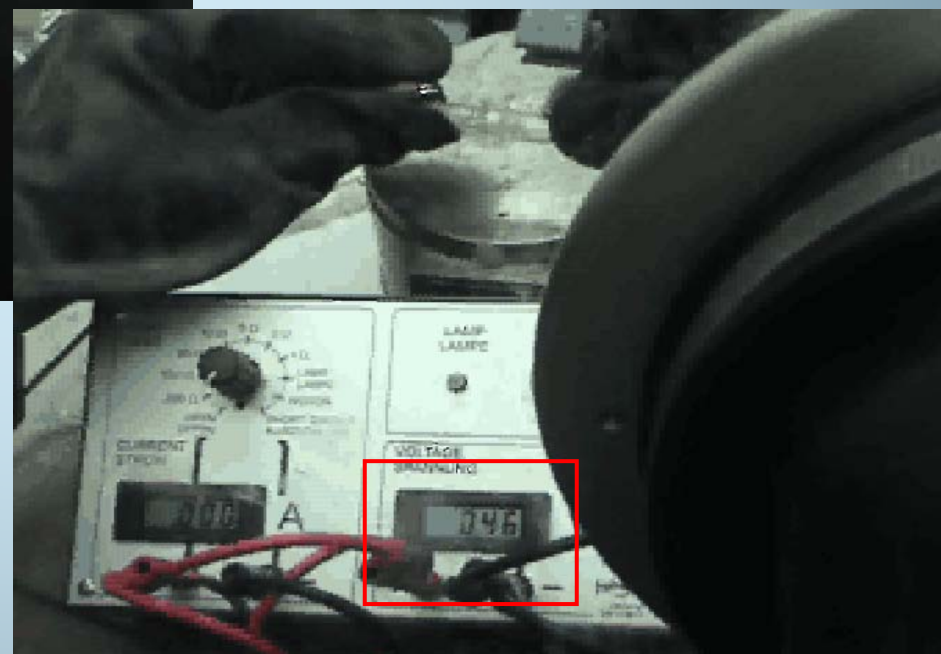

0.46 V / Unit Cell

Fe-Co Bionanobattery Cell – Solid Electrodes

Thiolated $Fe^{2+} \Longrightarrow$ thiolated Co^{3+}

0.25 V / Unit Cell

Estimation of Electrical Output

- Electrode: 1”x1” gold films coated on both sides of a quartz slide
- Total number of ferritin on each layer of 1” x 1” area: 4.48×10^{12}
- Total available electrons: 2×10^{16} per layer = 3.2×10^{-3} Coulomb
- Charge Density per Electrode (2×10^5 layers): 640 Coulomb
- Cell Charge Density (array of 10 electrodes): 6400 Coulomb
- Operational Run-time: 6400 seconds when Fe^{2+}-Co^{3+} electrodes discharge 1 C/sec
- If we connect 10 gold electrodes together, then
  - Parallel connection: 0.79 V, 1 A (2844 mWh)
  - Serial connection: 7.9 V, 100 mA

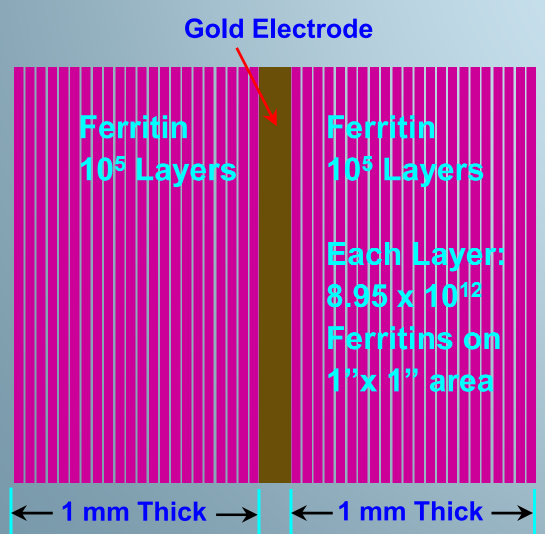

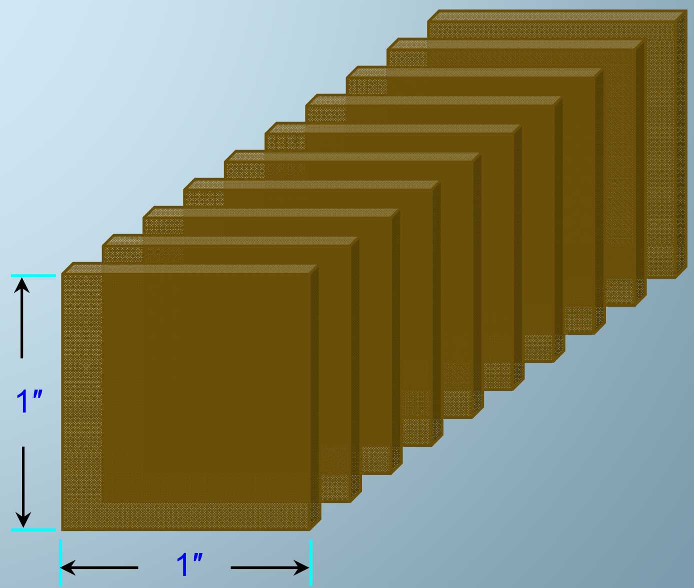

Conclusion

The areas discussed are still under development.

- Nano structured materials for TE applications
  - SiGe and Be-Te
  - Nano particles and nanoshells
- Quantum technology for optical devices
  - Quantum apertures
  - Smart optical materials
  - Micro spectrometer
- Bio-template oriented materials
  - Bionanobattery
  - Biofuel cells
  - Energetic materials